Virology 623 (2026) 111012

Contents lists available at ScienceDirect

Virology

journal homepage: www.elsevier.com/locate/virology

Mechanistic insights into flavonoid-mediated regulation of human influenza virus replication

Dibakar Chowdhury [a,b], Hillary A. Vanderven [a,b,c], Phurpa Wangchuk [d,e], Subir Sarker [a,b,f,*]

[a] Biomedical Sciences & Molecular Biology, College of Medicine and Dentistry, James Cook University, Townsville, QLD, 4811, Australia
[b] Australian Institute of Tropical Health and Medicine, James Cook University, Townsville, QLD, 4811, Australia
[c] Department of Microbiology and Immunology, Peter Doherty Institute for Infection and Immunity, The University of Melbourne, Parkville, VIC, 3010, Australia
[d] College of Science and Engineering, James Cook University, Nguma Bada Campus, McGregor Rd, Smithfield, Cairns, QLD, 4878, Australia
[e] Australian Institute of Tropical Health and Medicine, James Cook University, Cairns, QLD, 4878, Australia
[f] Department of Microbiology, Anatomy, Physiology and Pharmacology, School of Agriculture, Biomedicine and Environment, La Trobe University, Melbourne, Victoria, 3086, Australia

ARTICLE INFO

Keywords:
Influenza A virus
Flavonoid
Phytochemical
Replication
Drug discovery

ABSTRACT

Influenza A virus (IAV) remains a major global health concern due to its rapid mutation rate, antigenic variability, and the emergence of resistance to frontline antivirals such as oseltamivir and zanamivir. Despite available vaccines and therapeutics, their limited efficacy against emerging strains underscores the urgent need for new antiviral approaches. Therefore, plant-derived bioactive compounds, particularly flavonoids, have gained attention for their ability to target both viral and host pathways, yet their mechanisms of action remain incompletely understood. This review synthesises current evidence on the antiviral potential of plant-derived flavonoid against human IAV subtypes H1N1 and H3N2. Flavonoids disrupt key stages of the viral life cycle, including attachment, entry and release, and interact with IAV proteins such as hemagglutinin (HA), neuraminidase (NA), nucleoprotein (NP), and matrix-2 (M2) ion channels. The ability of plant-derived compounds to inhibit viral replication underscores their potential as leads for next-generation influenza therapeutics. Nonetheless, rigorous *in vivo* studies, mechanistic elucidation, and pharmacokinetic evaluations are essential to advance these candidates toward clinical translation.

1. Introduction

According to the World Health Organization, IAV persists in being a perpetual and evolving global health challenge, contributing to an approximated 3–5 million cases of severe illness and 290,000–650,000 respiratory-related deaths annually (WHO, 2025). As a highly contagious respiratory pathogen, IAV is responsible for recurrent seasonal epidemics and sporadic pandemics, posing significant morbidity and mortality risks to humans, livestock, and wildlife, alongside substantial economic burdens due to healthcare costs and productivity losses. The segmented, negative-sense RNA genome of IAV allows for frequent mutations and genetic reassortment via antigenic drift and shift, enabling the virus to evade host immunity and limiting the long-term effectiveness of current vaccines and therapeutics (Shanks, 2015; Su et al., 2017).

While neuraminidase inhibitors (NAI) such as oseltamivir, peramivir, laninamivir, and zanamivir remain widely used, their effectiveness could be compromised by the emergence of drug-resistant viral strains, although such resistance remains relatively uncommon (Beigel and Hayden, 2021). Another limitation of NAI is that they must be administered within approximately 48 h of symptom onset to be most effective (Orders, 2024). *Baloxavir marboxil*, a more recently authorised inhibitor targeting the IAV cap-dependent endonuclease, introduces a novel antiviral mechanism; nevertheless, cases of resistance emerged soon after its clinical introduction (Ison et al., 2021). Furthermore, antivirals targeting the M2 ion channel (rimantadine and amantadine) have largely been phased out due to widespread resistance among circulating IAV strains (Raza and Ashraf, 2024). These challenges underscore a pressing need for innovative antiviral approaches against influenza infection that can overcome resistance and improve treatment

This article is part of a special issue entitled: Invited Reviews 2026 published in Virology.

* Corresponding author. Biomedical Sciences & Molecular Biology, College of Medicine and Dentistry, James Cook University, Townsville, QLD, 4811, Australia.
E-mail address: subir.sarker@jcu.edu.au (S. Sarker).

https://doi.org/10.1016/j.virol.2026.111012
Received 20 February 2026; Received in revised form 26 May 2026; Accepted 16 June 2026
Available online 17 June 2026
0042-6822/© 2026 The Author(s). Published by Elsevier Inc. This is an open access article under the CC BY license (http://creativecommons.org/licenses/by/4.0/).

effectiveness.

Phytochemicals have gained recognition due to their plethora of therapeutic properties to inactivate and inhibit viral replication and modulate host immune responses. Historically rooted in traditional medicinal systems across Asia, including Traditional Chinese Medicine, Ayurveda, and Kampo—many plant-based therapies have demonstrated antiviral potential. Oseltamivir itself is a semi-synthetic derivative of shikimic acid, a plant compound extracted from *Illicium verum* (star anise), exemplifying the translational value of phytochemicals in modern antiviral drug development (El Sayed, 2000; Kim and Park, 2012). Plant-based compounds offer several advantages over conventional antivirals. Their structural diversity enables a broad range of biological activities, including interference with host pathways critical to viral replication. Among those, flavonoids are a diverse group of plant-derived compounds widely present in fruits and vegetables, recognised for their broad pharmacological activities, including antiviral effects (Sadati et al., 2019). Naturally occurring flavonoids, highly diversified plant pigments with polyphenolic structures, are found in numerous sources such as tea, wine, fruits, vegetables, grains, and various plant parts including bark, roots, stems, and flowers (Middleton Jr, 1998). Notable flavonoids with demonstrated antiviral activity include quercetin, apigenin, kaempferol, and baicalein (Bahramsoltani et al., 2016; Kumar and Pandey, 2013). The richness of flavonoid structural diversity, the extensive mechanistic and clinical evidence base exceeding 120,000 studies indexed in PubMed, and their recognised translational potential in drug discovery collectively justify the specific focus of this review on the anti-IAV activity of flavonoids, with particular emphasis on circulating human IAV subtypes H1N1 and H3N2, within the broader landscape of phytochemical compounds (Intharuksa et al., 2024).

This review explores the molecular basis by which plant-derived flavonoid compounds modulate IAV replication. By highlighting their antiviral activities and interactions, we emphasize their potential as promising leads for the development of next generation influenza therapeutics.

2. Definition and classification of flavonoids

Flavonoids are a large and structurally diverse class of naturally occurring plant secondary metabolites that belong to the polyphenol superfamily. Chemically, they are defined by a common *C6–C3–C6* diphenylpropane carbon skeleton, consisting of two aromatic benzene rings, designated ring A (the resorcinol moiety) and ring B (the catechol or phenyl moiety), interconnected by a three-carbon bridge that typically cyclises to form an oxygenated heterocyclic ring, referred to as ring C (the pyran ring) (Kumar and Pandey, 2013). The remarkable structural diversity observed across flavonoid compounds arises from variations in the degree of hydroxylation, methoxylation, glycosylation, and prenylation of this core scaffold, as well as differences in the position of ring B attachment and the oxidation state of ring C (Kumar and Pandey, 2013; Panche et al., 2016).

Based on the position of attachment of ring B to the flavan nucleus, the degree of unsaturation of ring C, and the oxidation pattern of the carbon skeleton, flavonoids are systematically classified into six major subclasses: flavones, flavonols, flavanones, flavanols (catechins), anthocyanidins, and isoflavones (Kumar and Pandey, 2013; Panche et al., 2016; Rauter et al., 2018). Minor subclasses, including neoflavonoids and chalcones, are also recognised. A key structural distinction lies in the position of ring B attachment: flavones, flavonols, flavanones, and flavanols all bear ring B at position 2 of ring C; isoflavones bear ring B at position 3; and neoflavonoids at position 4 (Panche et al., 2016; Rauter et al., 2018).

2.1. Modulation of IAV attachment

A major antiviral constituent of *Rumex acetosa* L. (known as sorrel) is procyanidin, a flavonoid whose activity is enhanced by the presence of galloyl groups (Derksen et al., 2014). Among the procyanidin derivatives, procyanidin B2-di-gallate demonstrated strong anti-influenza activity, with a 50% inhibitory concentration (IC_{50}) of approximately 15 μM [Fig. 1, Tables 1 and 2] (Derksen et al., 2014). Supporting this, Yang et al. reported that procyanidin B2 also significantly suppressed IAV replication in Madin–Darby canine kidney (MDCK) cells (Yang et al., 2014). However, contrasting findings were presented by Derksen et al., who observed no antiviral effect of procyanidin-B2 at non-cytotoxic concentrations. This inconsistency is likely due to methodological variations. Derksen and colleagues employed both the 3-(4, 5-Dimethylthiazol-2-yl)-2,5-Diphenyltetrazolium Bromide assay (MTT-based assay), where IAV and the compound were co-inoculated, and a plaque reduction assay (PRA), whereas Yang et al. utilized cytopathic effect (CPE) inhibition assays (Derksen et al., 2014; Yang et al., 2014). The initial phase of IAV infection is characterized by a highly specific interaction between the viral HA glycoprotein and terminal sialic acid moieties located on glycoproteins and glycolipids of the host cell surface. This binding event is critical for viral attachment, as the affinity and specificity of HA for α-2,3- or α-2,6-linked sialic acids largely determine host range and tissue tropism. By anchoring the virion to the cell membrane, HA-sialic acid interactions establish the foundation for subsequent internalisation through endocytic pathways, thereby initiating the infectious cycle (Dou et al., 2018). Mechanistic studies revealed that procyanidin B2-di-gallate interacts directly with the HA protein of IAV. Computational modelling suggested a strong binding affinity to the sialic acid recognition site of HA, potentially interfering with viral attachment to host cells (Derksen et al., 2014; Tian et al., 2020). Nevertheless, hemagglutination inhibition (HI) assays showed that the compound did not block IAV binding to HA. At higher concentrations (≥39 μM), it instead caused direct red blood cell agglutination, which cannot be regarded as genuine antiviral activity. Despite this, in assays such as MTT-based assay and PRA, procyanidin B2-di-gallate consistently inhibited IAV replication at low, non-toxic concentrations, suggesting an entry-stage mechanism of action. These findings highlight procyanidin B2-di-gallate and other galloylated procyanidins from *R. acetosa* as promising candidates for influenza prevention. However, a key limitation is their poor oral bioavailability, which makes systemic use impractical. Instead, localized delivery to the upper respiratory tract—through formulations such as lozenges, chewing gums, or inhalation—may be more effective, allowing direct interaction with the virus at its entry site (Derksen et al., 2014; Zumdick et al., 2012).

A study demonstrated that both 6-prenylnaringenin (6-PN) and 8-prenylnaringenin (8-PN) exhibited stronger anti-IAV activity than non-prenylated naringenin. 8-PN showed stronger inhibitory effects during the viral adsorption/entry stage (−1 to 0 h post-infection), suggesting interference with early events such as viral attachment or entry into host cells. 8-PN also displayed higher intracellular retention and slower efflux, which may contribute to its stronger early antiviral effects (Morimoto et al., 2022). In contrast, another study from same research group provided evidence showing that 8-PN inhibits both viral adsorption/entry (−1 to 0 h) and late-stage replication (4–8 h post-infection) processes across multiple IAV strains of H1N1 and H3N2, including oseltamivir-resistant IAV. Collectively, these findings suggest that 8-PN exerts broad anti-IAV activity through multi-stage inhibition associated with its prenylated structure (Fig. 2) (Hanada et al., 2022). A recent study demonstrated that amentoflavone, a biflavonoid compound, exhibits potent anti-IAV activity at half maximal effective concentration (EC_{50}) of 23.01 ± 0.07 μM by targeting multiple stages of the viral replication in RAW 264.7 cells. The compound inhibited viral attachment through interference with HA, exerted direct virucidal effects, and suppressed NA activity, thereby affecting both viral entry and progeny release. Additionally, amentoflavone reduced the expression of multiple IAV proteins, including NP, HA, NA, non-structural protein-1 (NS1), and polymerase basic 2 (PB2), and showed antiviral activity against H1N1

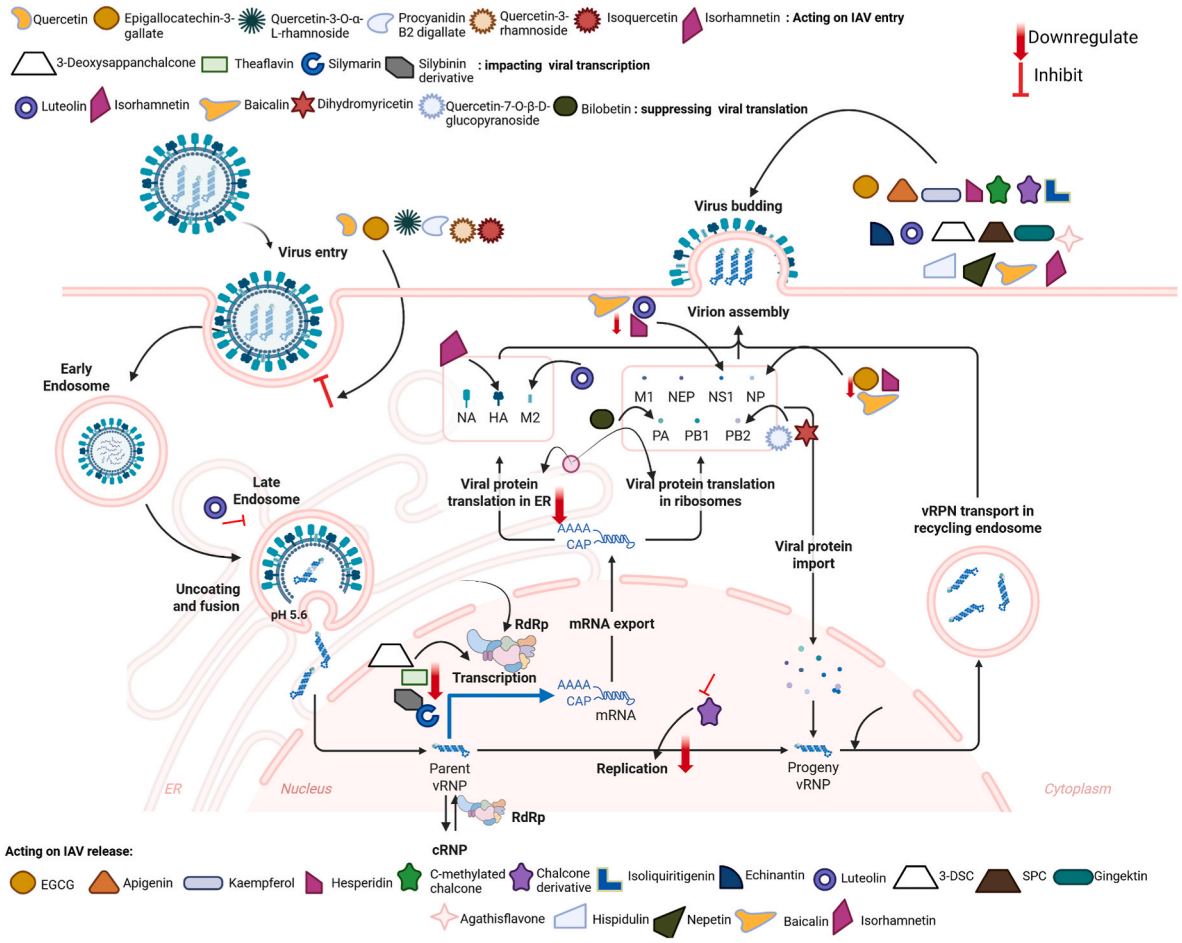


Fig. 1. Diagrammatic illustration of the inhibitory activities of plant-derived flavonoid compounds on different phases of IAV replication. The figure illustrates how flavonoids target viral entry, attachment, fusion uncoating, RNA transcription, replication, assembly and budding of influenza virus replication [Created in https://BioRender.com]. Abbreviations: PBD, Procyanidin B2-di-gallate; EGCG, Epigallocatechin gallate; Q7G, Quercetin-7-O-glucoside; Q3R, Quercetin3-rhamnoside; Q3L, Quercetin-3-O-α-L-rhamnopyranoside; TF, Theaflavin & Theaflavin-3′-gallate; S3, 23-(S)-2-amino-3-phenylpropanoyl-silybin; 3-DSC, 3-deoxy-sappanchalcone; SPC, sappanchalcone; HA, hemagglutinin; NA, neuraminidase; M1, matrix-1; M2, Matrix-2; NEP, nuclear export Protein; NS1, non-structural protein-1; NP, nucleoprotein; PA, polymerase acid; PB1, polymerase Basic 1; PB2, polymerase Basic 2, vRNP, viral ribonucleoprotein; cRNP, complementary ribo-nucleoprotein; RdRp, RNA dependent RNA polymerase.

and H3N2, supporting its broad-spectrum antiviral potential (Cho et al., 2024).

A flavonoid glycoside, quercetin-3-O-α-L-rhamnopyranoside (Q3L) isolated from *Rapanea melanophloeos* (Dwarf cape beach), acted by disrupting virus particle–cell receptor interactions [Fig. 1, Tables 1 and 2]. In co-treatment assays where MDCK cells were exposed to IAV and the compound simultaneously, a marked reduction in M and NP gene expression was observed. In contrast, pre-treatment and post-infection treatments had little or no effect on these viral genes (Mehrbod et al., 2018). Similarly, quercetin 3-rhamnoside (Q3R) from *Houttuynia cordata* (fish mint) potently inhibited A/WS/33 infection [Figs. 1 and 2, Tables 1 and 2], reducing CPE in MDCK cells and blocking at the entry stage through indirect interactions with viral particles, as confirmed by time-of-addition assays (Choi et al., 2009).

Together, these studies indicate that procyanidin B2-di-gallate, Q3L, and Q3R primarily exert their antiviral effects during the viral attachment phase, either by directly interacting with HA or indirectly interfering with particle–cell binding. Such entry-stage inhibition underscores their potential as preventive agents targeting the earliest step of IAV infection.

2.2. Interruption of IAV internalisation

Luteolin, a flavonoid compound, exhibited strong antiviral activity against H3N2 and H1N1 IAVs in MDCK cells, with IC_{50} values of 6.89 μM and 7.15 μM, respectively [Fig. 1, Table 2]. Both qRT-PCR and immunofluorescence assays (IFA) confirmed that luteolin significantly reduced viral M2 mRNA and protein levels in a concentration-dependent manner. Time-of-addition experiments further revealed that luteolin was most effective between −2 and 4 h post-infection, coinciding with early stages of viral replication, as evidenced by reduced M2 mRNA expression. Importantly, HI assays and viral pre-treatment studies indicated that luteolin does not directly bind to viral particles or block hemagglutination. Instead, Western blot analysis showed that luteolin decreased the expression of viral NS1 protein as well as Coat Protein Complex I (COPI) components in H1N1 and H3N2 IAV-infected MDCK, Vero, and Calu-3 (human lung carcinoma) cells (Yan et al., 2019). Influenza internalisation refers to the process by which influenza virus particles are taken up into the host cell, usually via clathrin-mediated endocytosis or other endocytic pathways (Dou et al., 2018). The COPI complex is essential for endocytic trafficking and influenza virus entry, with the β-COP subunit playing a key role in vesicular transport between the Golgi apparatus and endoplasmic reticulum, while also facilitating viral internalisation (Beck et al., 2009; Cureton et al., 2012; Gabriely et al., 2007). Luteolin downregulated β-COP expression, thereby disrupting viral internalisation, consistent with its inhibitory effects during the entry stage of influenza infection (Yan et al., 2019).

Epigallocatechin gallate (EGCG), a flavonoid abundant in green tea,

Table 1
List of flavonoid compounds acting on IAV replication.

Compound	Source Plant	Classification	Action on virus	Reference
Procyanidin B2-di-gallate	*Rumex acetosa* L.	Flavonoid	inhibits viral entry, interact with hemagglutination	Derksen et al. (2014)
Procyanidin B2	*Camellia sinensis* (L.) Kuntze (Black tea)	Flavonoid	may reduce IAV replication	Yang et al. (2014)
Luteolin	*Petroselinum crispum* (Mill.) Fuss, *Elsholtzia rugulosa* Hemsl.	Flavone	may inhibit viral fusion and inhibit NA activity	(Liu et al., 2008; Yan et al., 2019)
Dihydromyricetin	*Ampelopsis grossedentata* (Hand-Mazz.) J.Wen & Z.L.Nie	Flavanonol	interfere with viral ribonucleoprotein (vRNP)function targeting PB2 subunit	Tian et al. (2020)
Cirsimaritin (CST)	*Artemisia scoparia* Maxim.	Flavone	Interfere with viral entry stage	Yan et al. (2018)
Quercetin	*Eupatorium fortunei* Turcz.	Flavanoid	suppress M2 protein and gene transcription	(Chen et al., 2012; Choi et al., 2017; Wu et al., 2015)
Quercetin-7-O-glucoside	*Dianthus superbus* L.	Flavanoid glycoside	inhibit mRNA synthesis of replication and may target PB2	Gansukh et al. (2016)
Quercetin 3-rhamnoside (Q3R)	*Houttuynia cordata* Thunb.	Flavonol glycoside	inhibit entry stage	Choi et al. (2009)
Quercetin-3-O-α-L-rhamnopyranoside (Q3L)	*Rapanea melanophloeos* (L.) Mez	Flavonol glycoside	disrupt viral particle-cell receptor interaction	Mehrbod et al. (2018)
Isoquercetin	*Camellia sinensis* (L.) Kuntze (Black tea)	Flavonol glycoside	may act on entry stage	Kim et al. (2010)
Bilobetin	*Euphorbia brevicornu Pax*	Biflavonoid	inhibit polymerase acidic (PA) activity	Zhang and Wang (2021)
Theaflavin (TF1)	*Camellia sinensis* (L.) Kuntze (Black tea)	Flavonol dimer	inhibit viral transcription and reduce NP expression	Sima et al. (2023)
Theaflavin-3′-gallate (TF2b)	*Camellia sinensis* (L.) Kuntze (Black tea)	Flavonol dimer	inhibit viral transcription and reduce NP expression	Sima et al. (2023)
Silybin derivative [23-(S)-2-amino-3-phenylpropanoyl-silybin (S3)]	*Silybum marianum L.* (Milk thistle)	Flavonolignan	May interfere with vRNP	Dai et al. (2013)
Silibinin	*Silybum marianum L.* (Milk thistle)	Flavonolignan	inhibition of viral RNA synthesis	Keshavarz et al. (2025)
Silymarin	*Silybum marianum L.* (Milk thistle)	Flavonolignan complex	may inhibit viral RNA synthesis	Song and Choi (2011)
Epigallocatechin gallate (EGCG)	*Camellia sinensis* (L.) Kuntze (Black tea)	Flavanoid	inhibit viral fusion	Mou et al. (2020)
(−)-epigallocatechin-3-gallate	*Camellia sinensis* (L.) Kuntze (Black tea)	Flavanoid	inhibit viral entry and internalisation	(Colpitts and Schang, 2014; Kim et al., 2013; Xu et al., 2017)
Apigenin	*Elsholtzia rugulosa* Hemsl.	Flavone	NA inhibition	(Liu et al., 2008; Xu et al., 2020)
Kaempferol	*Elsholtzia rugulosa* Hemsl.	Flavonol	suppress replication without affecting viral adsorption or entry	Dong et al. (2014)
Hesperidin	*Citrus maxima* (Burm.) Merr.	Flavonone glycoside	Suppress NS1 and NP expression	Dong et al. (2014)
Tricin	*Sasa senanensis* (Franch. & Sav.) Rehder		may interfere with viral entry and fusion	Yazawa et al. (2011)
C-methylated flavonoids	*Cleistocalyx operculatus* (Roxb.) Merr. & L.M.Perry	Chalcone type flavonoid	inhibit NA activity	Dao et al. (2010)
Miquelianin (quercetin 3-O-glucuronide)	*Bupleurum chinense* DC. *Nelumbo nucifera* Gaertn	Flavonol glycoside	inhibit nuclear export of vRNP	Li et al. (2025)
Isorhamnetin	*Ginkgo biloba* L. & *Hippophaerhamnoides* L.	Flavanol	inhibit HA & NA	Dayem et al. (2015)
Baicalin	*Scutellaria baicalensis* Georgi	Flavone glucuronide	suppress NP, inhibit NA and bind to NS1	(Ding et al., 2014; Nayak et al., 2014)

has been shown to inhibit the cellular entry of H1N1 IAV subtypes, with half-maximal effective concentration (EC_{50}) values ranging from 5.7 to 17.3 μM in MDCK cells and 24 to 26 μM in CaLu-3 cells [Fig. 1 & Table 2] (Kim et al., 2013; Müller and Downard, 2015; Stannard et al., 2023). Multiple studies indicate that EGCG primarily targets an early stage of the viral life cycle. Although it does not interfere with HA or polymerase activity, EGCG compromises viral envelope integrity, preventing hemifusion with host membranes and thereby blocking viral internalisation after attachment. Despite its potent *in vitro* activity, *in vivo* outcomes have been variable. In BALB/c mice infected with influenza virus, oral administration of EGCG at 40 mg/kg/day improved survival, lowered viral titers, and alleviated pneumonia, with effects comparable to oseltamivir. However, no protection was observed at 10 mg/kg/day (Ling et al., 2012). In contrast, ferret models infected with H1N1 IAV subtypes showed no measurable antiviral benefits, even with high doses of EGCG (500 mg/kg/day, twice daily). These discrepancies highlight the importance of pharmacokinetic investigations to clarify systemic distribution and tissue exposure (Stannard et al., 2023).

Overall, both luteolin and EGCG interfere with the internalisation phase of IAV infection, albeit through distinct mechanisms—luteolin by downregulating COPI components critical for endocytosis, and EGCG by destabilizing the viral envelope to prevent hemifusion. These findings underscore the potential of flavonoids as early-stage inhibitors, though their variable *in vivo* efficacy highlights the need for pharmacokinetic optimisation.

2.3. Inhibition of IAV fusion

Following the internalisation of IAV, endosomal acidification induces conformational changes in HA, exposing the fusion peptide of the HA2 subunit, which drives merging of the viral envelope with the endosomal membrane (Dou et al., 2018). Quercetin, a widely studied flavonoid, demonstrated broad-spectrum inhibitory activity against IAV, with IC_{50} values of approximately 27 μM for H1N1 A/PR/8/34, 22 μM for H1N1 A/FM/1/47, and 10 μM for H3N2 A/Aichi/2/68 [Table 2]. Functional assays, including time-of-addition, surface plasma resonance (SPR), and microscale thermophoresis (MTS) assays—revealed that quercetin interacts with the HA2 subunit [Tables 1 and 2], thereby

Table 2
In vitro anti-influenza activity against diverse H1N1 and H3N2 strains.

Compound	Model	strain	IC50	EC50	CC50	SI	Reference
Procyanidin B2-di-gallate	MDCK	A/Puerto Rico/8/34 (H1N1)	≤15 μM	NA	191 μM	12	Derksen et al. (2014)
Luteolin	MDCK	A/Jiangxi/312/2006 (H3N2)	NA	6.89 μM	148.43 μM	21.54	Yan et al. (2019)
		A/Fort Monmouth/1/1947 (H1N1)	NA	7.15 μM		20.76	
		A/Jinan/15/90 (H3N2)	2.06 μg/mL	NA	3.56 μg/mL	1.73	Liu et al. (2008)
Rhein	MDCK	A/ShanTou/169/06		1.51 μg/mL	64.59 μg/mL	42.77	
Dihydromyricetin	MDCK	A/Puerto Rico/8/34 (H1N1)	15.18 ± 0.92 μM	NA	505.518 ± 12.8 μM	33.27	Tian et al. (2020)
	MDCK	A/Aichi/2/68 (H3N2)	23.33 ± 4.83 μM	NA		21.7	
	MDCK	A/FM1/47 (H1N1)	11.67 ± 2.28 μM	NA		43.4	
Quercetin-7-O-glucoside (Q7G)	MDCK	A/Puerto Rico/8/34 (H1N1)	3.1 ± 0.43 μg/ml	NA	>100 μg/ml	32.25	Gansukh et al. (2016)
	MDCK	A/Vic/3/75 (H3N2)	6.61 ± 0.08 μg/ml		>100 μg/ml	15.19	
Isoquercetin	MDCK	A/swine/OH/511445/2007 (H1N1)	NA	1.2 μM	46 μM	38	Kim et al. (2010)
Theaflavin (TF1)	MDCK	Mouse adapted A/Changchun/01/2009 (H1N1)	NA	11.72 μg/mL	147.8 μg/mL	12.61	Sima et al. (2023)
Theaflavin-3′-gallate (TF2b)	MDCK	Mouse adapted A/Changchun/01/2009 (H1N1)		8.45 μg/mL	114.2 μg/mL	13.51	
23-(*S*)-2-amino-3-phenylpropanoyl-silybin (S3)	MDCK	A/ShanTou/169/06 (H1N1)	NA	2.36 ± 0.44 μM	>400 μM	169.58	Dai et al. (2013)
23-(S)-2-amino-4-methyl-pentanoyl-Silybin (S4)	MDCK			3.81 ± 0.52 μM		104.97	
23-(S)-2-aminopropanoyl-Silybin (S2)	MDCK			5.32 ± 1.16 μM		75.19	
Apigenin	MDCK	A/Puerto Rico/8/34 (H1N1)	1.340 μg/mL	NA	216.2 μg/mL	161	Wu et al. (2010)
		A/Jinan/15/90 (H3N2)	1.43 μg/mL	NA	10.69 μg/mL	7.48	Liu et al. (2008)
		Oseltamivir- and peramivir-resistant A/Toyama/129/2011 (H1N1)	NA	17.8 ± 8.7	66.7 ± 6.1 μg/mL	3.74	Kai et al. (2014)
		A/Toyama/129/2011 (H1N1)	NA	8.1 ± 4.7	>100 μg/mL	ND	Kai et al. (2014)
Kaempferol	MDCK	A/PR/8/34(H1N1)	NA	38.2 ± 17.1			Kai et al. (2014)
		Oseltamivir- and peramivir-resistant A/Toyama/129/2011 (H1N1)	NA	21.7 ± 5.5			Kai et al. (2014)
		A/Toyama/129/2011 (H1N1)	NA	24.8 ± 4.3			Kai et al. (2014)
5-hydroxy-6,7-dimethoxyflavone	MDCK	A/Puerto Rico/8/34 (H1N1)	2.194 μg/mL	NA	161.1 μg/mL	73.4	Wu et al. (2010)
5-hydroxy-7,8-dimethoxyflavone	MDCK	A/Puerto Rico/8/34 (H1N1)	2.322 μg/mL	NA	152.6 μg/mL	65.7	Wu et al. (2010)
Acacetin	MDCK	A/Puerto Rico/8/34 (H1N1)	1.671 μg/mL	NA	197.8 μg/mL	118	Wu et al. (2010)
Tricin	MDCK	A/Solomon islands/3/2006 (H1N1)	NA	4.6 μM	No cytotoxicity observed until 30 μM	ND	Yazawa et al. (2011)
		A/Hiroshima/52/2005 (H3N2)		3.4 μM		ND	Yazawa et al. (2011)
		A/Narita/1/2009 (H1N1pdm)		8.2 μM		ND	Yazawa et al. (2011)
		A/California/07/2009 (H1N1pdm)		10.2 μM		ND	Yazawa et al. (2011)
C-methylated flavonoid 4	MDCK	A/Puerto Rico/8/34 (H1N1)	NA	4.90 ± 0.35 μM	>120 μM μM	>24.49	Dao et al. (2010)
C-methylated flavonoid 7	MDCK	A/Puerto Rico/8/34 (H1N1)		7.72 ± 0.70 μM	78.39 ± 4.16 μM	10.15 ± 0.54	Dao et al. (2010)
C-methylated flavonoid 8	MDCK	A/Puerto Rico/8/34 (H1N1)		8.13 ± 0.81 μM	135.00 ± 5.81 μM	16.61 ± 0.71	Dao et al. (2010)
C-methylated flavonoid 14	MDCK	A/Puerto Rico/8/34 (H1N1)		8.79 ± 1.05 μM	>120 μM	>13.65	Dao et al. (2010)
3-Deoxysappanchalcone	MDCK	A/Guangdong/243/72 (H3N2)	1.06 μg/mL	NA	17.25 μg/mL	16.27	Liu et al. (2009)

(*continued on next page*)

Table 2 (*continued*)

Compound	Model	strain	IC50	EC50	CC50	SI	Reference
Sappanchalcone	MDCK	A/Guangdong/243/72 (H3N2) (H3N2)	2.06 μg/mL		12.83 μg/mL	6.23	Liu et al. (2009)
Baicalin	MDCK	A/FM1/1/47 (H1N1)	NA	43.3 μg/ml	373.5 μg/mL	8.6	Ding et al. (2014)
Baicalin		A/Beijing/32/92 (H3N2)		104.9 μg/ml		3.6	Ding et al. (2014)
Baicalin	A549	A/FM1/1/47 (H1N1)		40.3 μg/ml	215.2 μg/mL	5.3	Ding et al. (2014)
Baicalin		A/Beijing/32/92 (H3N2)		100.1 μg/ml		2.1	Ding et al. (2014)
Baicalin	A549	A/Jingfang/01/1986 (H1N1)		17.04 μg/mL	NA	NA	Li and Wang (2019)
Baicalin		A/Lufang/09/1993 (H3N2)		19.31 μg/mL	NA	NA	Li and Wang (2019)
Baicalin	MDCK	A/WSN/33 (H1N1)	7.4 μM	ND	ND	ND	Ji et al. (2015)
Baicalin	A549	A/California/07/2009 (H1N1)pdm09	18 μM				Nayak et al. (2014)
Baicalein	MDCK	A/WSN/33 (H1N1)	7.5 μM				Ji et al. (2015)
Wogonin	MDCK	A/WSN/33 (H1N1)	2.1 μM				Ji et al. (2015)
Chrysin	MDCK	A/WSN/33 (H1N1)	7.7 μM				Ji et al. (2015)
Oroxylin A	MDCK	A/WSN/33 (H1N1)	12.8 μM				Ji et al. (2015)
Epigallocatechin-3-O gallate (EGCG)	MDCK	A/Puerto Rico/8/34 (H1N1)	≤12 μM	NA	>200 μM	16	Derksen et al. (2014)
		A/Perth/25/2013		28.4 μM	280.1 μM	9.86	Müller and Downard (2015)
		A/Victoria/503/2013		29.0 μM	274.6 μM	9.46	Müller and Downard (2015)
	MDCK	A/Puerto Rico/8/34 (H1N1)	NA	10.0 ± 0.5 μM	195.8 ± 6.7 μM	19.6	Kim et al. (2013)
		A/Taiwan/1/1986 (H1N1)	NA	8.9 ± 0.6 μM	195.8 ± 6.7 μM	22	Kim et al. (2013)
		A/Brisbane/59/2007 (H1N1)		17.3 ± 3.2 μM	195.8 ± 6.7 μM	11.3	Kim et al. (2013)
		A/Hong Kong/8/68 (H3N2)		10.0 ± 2.3 μM	195.8 ± 6.7 μM	19.6	Kim et al. (2013)
		A/Korea/01/2009 (H1N1)		5.8 ± 0.5 μM	195.8 ± 6.7 μM	33.8	Kim et al. (2013)
		A/California/07/2009	3.0 μM	NA	290 μM	96	Stannard et al. (2023)
		A/Victoria/2570/2019	3.8 μM	NA	290 μM	77	Stannard et al. (2023)
		A/Yamagata/120/86 (H1N1)	NA	8.71 ± 1.11 nmol/L	81.18 ± 9.90 nmol/L	9.32	Ling et al. (2012)
	Calu-3	A/California/07/2009	24 μM	NA	420 μM	18	Stannard et al. (2023)
		A/Victoria/2570/2019	26 μM	NA	420 μM	16	Stannard et al. (2023)
Isorhamnetin	MDCK	A/Puerto Rico/8/34 (H1N1)	NA	23 μM	>280 μM	>17 μM	Dayem et al. (2015)
Miquelianin	MDCK	Mouse-adapted A/Changchun/01/2009 (H1N1)	NA	107.8 μM	143.9 μM		Li et al. (2025)
Taxifolin	MDCK	Mouse-adapted A/Changchun/01/2009 (H1N1)	NA	31.38 μM	56.65 μM		Li et al. (2025)
Daidzein	MDCK	A/Puerto Rico/8/34 (H1N1)	143.6 ± 78.9	NA	NA	>27	Morimoto et al. (2023)
Gossypetin	MDCK	A/Puerto Rico/8/34 (H1N1)	NA	43.0 μM	283.0 μM	6.58	Jeong et al. (2009)
Agathisflavone	MDCK	A/Puerto Rico/8/34 (H1N1)	NA	1.3 ± 0.5 μM	349 ± 17.5	268.46	de Freitas et al. (2020)
Hispidulin		A/Puerto Rico/8/34 (H1N1)		22.62 ± 1.79 μM	>200	>8.90 ± 0.76	Bang et al. (2016)
Nepetin				17.45 ± 0.54 μM	~200	~11.47 ± 0.37	Bang et al. (2016)
Diosmin	A549	A/Puerto Rico/8/34 (H1N1)	2.91 ± 3.22 μM	NA	11320.23 ± 2.29 μM		AbuBakar et al. (2025)
Licoflavone B	MDCK-Gluc	A/Puerto Rico/8/34 (H1N1)	6.7 μM	NA	100-200 μM	14.9-22.9	Fan et al. (2025)

(*continued on next page*)

Table 2 (*continued*)

Compound	Model	strain	IC50	EC50	CC50	SI	Reference
Rhamnocitrin	MDCK	H3N2	2.322 μM		>100 μM	>43	Chen et al. (2024)
Naringenin (Na)	MDCK	A/Puerto Rico/8/34 (H1N1)	290 ± 16.2 μM	NA	NA	4.9	Morimoto et al. (2022)
8-prenylnaringenin (8-PN)			24 ± 0.6 μM			4.9	
6-prenylnaringenin (6-PN)			38 ± 4.7 μM			5.5	
Cirsimaritin	MDCK	A/Fort Mon mouth /1/1947 (H1N1)	6.3 ± 1.4 μg/ml	NA	153.3 μg/ml	24.3	Yan et al. (2018)
		A/Tianjin Jinnan /15/2009 (H1N1)	5.8 ± .22 μg/ml	NA		26.4	
		A/JiangXi/312/2006 (H3N2)	11.1 ± 1.1 μg/ml	NA		13.8	

*IC_{50}: The concentration that inhibits viral replication or enzyme activity by 50%.
*EC_{50}: The concentration required to achieve 50% of the maximal antiviral effect.
*CC_{50}: The concentration of a compound that reduces cell viability by 50%.
*SI (Selectivity Index): The ratio of CC_{50} to EC_{50} or IC_{50}, reflecting the therapeutic index of the compound.

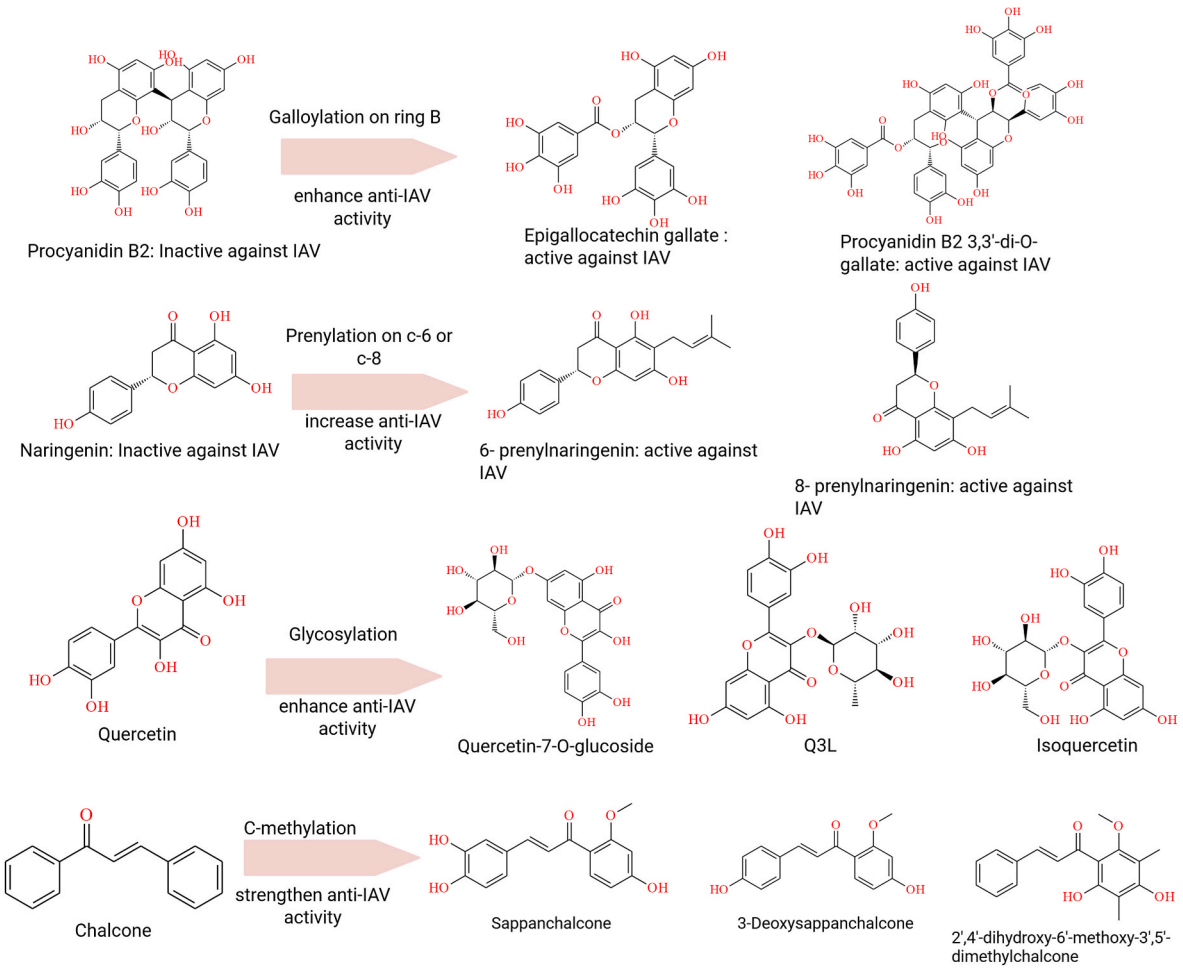


Fig. 2. Graphical overview of structure–activity relationships (SAR) of flavonoids against IAV. Four SAR themes are illustrated in the figure. Galloylation on ring B: Procyanidin B2 (inactive) gains anti-IAV activity upon galloylation, as demonstrated by epigallocatechin gallate and procyanidin B2 3,3′-di-O-gallate, both of which may interrupt viral entry stage. Prenylation at C-6 or C-8: Naringenin (inactive) acquires antiviral potency following prenylation at C-6 or C-8, with both derivatives inhibiting viral adsorption and entry. Glycosylation: Glycosidic modification of quercetin yields derivatives quercetin-7-O-glucoside (Q7G), quercetin-3-O-L-rhamnoside (Q3L), and isoquercetin each with distinct entry-stage inhibitory profiles. Chalcone derivatives: Sappanchalcone, 3-deoxysappanchalcone, and 2′,4′-dihydroxy-6′-methoxy-3′,5′-dimethylchalcone demonstrate that C-methylation on the chalcone scaffold confer neuraminidase inhibitory activity, including against oseltamivir-resistant IAV strains.

blocking viral fusion and acting directly on viral particles rather than host cells (Wu et al., 2015).

2.4. Suppression of IAV transcription, replication, and protein expression

The viral fusion event releases viral ribonucleoprotein complexes (vRNPs) into the host cell cytoplasm. The vRNPs are then transported to

the nucleus through the host importin-α/β pathway. Once inside the nucleus, the viral RNA-dependent RNA polymerase (RdRp) complex initiates transcription and replication of the segmented negative-sense RNA genome (Dou et al., 2018). The polymerase basic 2 (PB2) subunit of the viral RNA polymerase complex is essential for the "cap-snatching" process, required for viral mRNA transcription. Its cap-binding domain (residues 318–483) is highly conserved and structurally distinct from host proteins, making it an attractive antiviral target (Liu et al., 2013; Tian et al., 2020). Dihydromyricetin, a natural flavonoid from *Ampelopsis grossedentata* (Vine tea), displayed strong inhibitory activity against H1N1 and H3N2 IAV subtypes in MDCK cells, with IC_{50} values ranging from 11.67 to 23.33 μM [Table 2]. Mechanistic studies revealed that dihydromyricetin binds specifically to PB2, disrupting vRNP function without affecting other stages of the viral life cycle, such as entry or release [Fig. 1, Tables 1 and 3]. Supporting this, SPR and molecular docking analyses confirmed that dihydromyricetin targets the PB2 cap-binding pocket, competing with host-derived caps (Tian et al., 2020). Therefore, dihydromyricetin could be a potential antiviral candidate to enhance therapeutic efficacy against influenza virus infections.

Several studies have explored flavonolignan derivatives from *Silybum marianum* (Milk thistle) as potential inhibitors that can interfere with post-fusion stages of the IAV life cycle [Table 1]. The anti-IAV potential of silybin derivatives has been explored in MDCK cells, where S3 [23-(S)-2-amino-3-phenylpropanoyl-silybin] exhibited potent activity against H1N1 IAV, with an EC_{50} of 2.36 μM. In plaque inhibition assays, S3 was more effective than the parent compound (S0) and outperformed ribavirin at 80 μM [Table 2]. Time-course analyses indicated that S3 primarily acts during the viral entry stage (1–4 h post-infection). However, since immunoblotting, qRT-PCR, and IFA assays also showed marked suppression of NP expression, S3 may not only interfere with viral entry but could also affect subsequent transcription or translation processes, although the study did not explicitly clarify this mechanism. [Fig. 1]. *In vivo*, S3 significantly reduced viral replication and mortality, although lung viral titers were not measured [Table 4] (Dai et al., 2013). Future investigations should evaluate its pharmacokinetics, lung viral load, safety profile, and further validate the mechanism of NP suppression to establish therapeutic potential. Silibinin, another flavonolignan from a plant known as milk thistle, reduced lung tissue damage in BALB/c mice following H1N1 infection [Table 4]. While pretreatment at both low and high doses did not alter viral titers, post-treatment with a high dose significantly lowered viral load in bronchoalveolar lavage fluid (BALF), whereas the low dose remained ineffective (Keshavarz et al., 2025). Additionally, silymarin, a flavonolignan complex from the milk thistle, displayed strong *in vitro* activity against A/PR/8/34, reducing CPE by 98% at 100 μg/mL without cytotoxicity [Fig. 1]. RT-PCR analyses suggested inhibition of viral RNA synthesis, comparable to oseltamivir, highlighting its potential for further *in vivo* evaluation (Song and Choi, 2011).

Cirsimaritin (CST), a flavonoid isolated from *Artemisia scoparia* (Wormwood), suppressed H1N1 and H3N2 IAV replication in MDCK cells and a human monocytic leukemia cell line (THP-1) by reducing M2 RNA and protein expression in a dose-dependent manner [Fig. 1 & Table 1], as shown by qRT-PCR and IFA. HI and NA inhibition (NAI) assays indicated no effect on viral attachment or release, though time-of-addition studies were not performed. Western blot analysis suggested that CST's antiviral activity may involve inhibition of the nuclear factor kappa B/p65 subunit (NF-κB/p65) signalling pathway which is normally required for efficient transcription/replication of viral RNA and viral protein accumulation (Yan et al., 2018). Therefore, CST has potential for development as an anti-IAV agent or complementary therapy (Yan et al., 2018). Further studies should include detailed time-of-addition and *in vivo* experiments to clarify the precise stage and relevance of CST-mediated inhibition. A recent study identified diosmin as a promising anti-IAV flavonoid with potent activity against IAV (H1N1) in human lung adenocarcinoma cell (A549). Diosmin inhibited both viral attachment and post-entry replication stages, reduced viral protein expression, and modulated host antiviral immune responses through enhancement of type I interferon signalling [Table 1]. Notably, the compound exhibited its strongest antiviral effect during the post-entry stage, with an IC_{50} value of 12.17 ± 1.55 μM, indicating significant suppression of intracellular viral replication processes. Molecular docking further suggested strong interactions with key viral proteins, including HA, neuraminidase NA, and NS1, supporting its multi-target antiviral potential. Further mechanistic investigations, including *in vivo* study and combination studies with existing antivirals, may help clarify its therapeutic applicability and potential synergistic effects [Table 3] (AbuBakar et al., 2025).

Beyond quercetin itself, several of its derivatives exhibit enhanced potency. For instance, quercetin-7-O-glucoside (Q7G) displayed strong antiviral activity, with IC_{50} values of 3.1 μg/mL against A/PR/8/34 and 6.61 μg/mL against A/Vic/3/75H1N1 IAVs [Tables 1 and 2]. Time-course experiments showed that Q7G (10 μg/mL) was highly effective during the first 2 h post-infection but lost activity at later stages [Fig. 1].

Table 3
Summary of molecular docking studies of plant compounds against key IAV protein targets.

Compound	IAV Target	Binding Site/ Domain	Docking tool	Key Finding	Reference
Dihydromyricetin	PB2	Cap-binding domain (residues 318–483)	USCF Chimera system	Interacts with the PB2 cap-binding site via His432, His357, Phe404, Phe323, Glu361, Lys376, and Phe363 through π–π stacking, hydrophobic interactions, and hydrogen bonding.	Tian et al. (2020)
Baicalin	NS1	RNA-binding domain (residues 39–43)	PatchDock and GOLD v5.1	Baicalin interacted with NS1 residues Arg35, Arg38, Asp39, Gln40, Ser42, and Arg46, with predicted hydrogen bond formation involving Arg35, Arg38, and Arg46.	Nayak et al. (2014)
Quercetin-7-O-glucoside (Q7G)	PB2	Cap-binding pocket	AutoDockVina 1.1.2	Q7G interacted with PB2 residues His357, Phe323, Phe404, Lys376, Glu361, Ser321, Ser324, Arg332, His342, and Met431 through aromatic stacking and hydrogen bonding interactions.	Gansukh et al. (2016)
Licoflavone B	RdRp complex	Polymerase complex binding site	Discovery Studio 2016	Licoflavone B binds most favorably to Site 2 of the PA subunit within the influenza RdRp complex, with hydrogen bond interactions identified between the compound and backbone residues of the polymerase	
Diosmin	HA, NA, NS1	Multiple binding sites	AutoDock Vina (version 1.1.2)	Diosmin exhibited the strongest docking affinity toward NS1 and HA, mediated by extensive hydrogen bonding, van der Waals, π–π, and polar interactions, highlighting its potential antiviral flavonoid.	AbuBakar et al. (2025)
Procyanidin B2-di-gallate, EGCG	HA	Sialic acid recognition site	Molecular Operating Environment (MOE) version 2011.10	Docking analysis showed deep insertion of the galloyl groups into the sialic acid-binding pocket, indicating stronger binding and enhanced antiviral activity of the galloylated compound compared with ungalloylated molecules.	Derksen et al. (2014)

Table 4
Summarized list of flavonoid compounds evaluated in *in vivo* animal models against IAV infection.

Compound	Animalmodel	IAV Strain	Route and dose	Key *in vivo* finding	Reference
EGCG (epigallocatechin gallate)	BALB/c mice; ferret	Mice:10 LD_{50} of A/FM1/47 (H1N1) Ferret: 1×10^5 $TCID_{50}$ A/California/07/2009 (H1N1pdm09)	Oral; 10, 20 or 40 mg/kg/day for 5 days(mice); 250 mg/kg/day twice daily for 4 days (ferret)	40 mg/kg/day improved survival, lowered viral titres, and alleviated pneumonia comparable to oseltamivir; no antiviral benefit observed in ferret model at any dose tested	(Ling et al., 2012; Stannard et al., 2023)
23-(S)-2-amino-3-phenylpropanoyl-silybin (S3)	BALB/c mice	5 MLD_{50} of A/PR8	Oral gavage; 25 mg/kg/day for 10 days	Significantly reduced viral replication and mortality compared to untreated controls	Dai et al. (2013)
Silibinin	BALB/c mice	5 LD_{50} of A/Puerto Rico/8/34 (H1N1)	Intraperitoneal route; Low (25 mg/kg) and high (50 mg/kg) dose; for 7days	Post-treatment with high dose significantly lowered viral load in BALF and reduced lung tissue damage; pretreatment at either dose did not alter viral titres	Keshavarz et al. (2025)
Isoquercetin	BALB/c mice	1 LD_{50} of A/Puerto Rico/8/34 (H1N1)	Intraperitoneal; 10 mg/kg/day for 6 days	Reduced lung viral titres compared to untreated controls	Kim et al. (2010)
Tricin	DBA/2Cr mice	1600 PFU of A/Puerto Rico/8/34 (H1N1)	Oral gavage; 20 or 100 μg/kg for five days	Significantly reduced body weight loss and prolonged survival compared to controls	Yazawa et al. (2011)
Baicalin	BALB/c mice; ICR mice	BALB/c: 4 MLD_{50} of A/California/07/2009 (H1N1pdm09) ICR mice: 50 MLD_{50} of A/FM1/1/47 (H1N1)	BALB/c: Oral gavage; 10-120 mg/kg/day twice for 3 days ICR mice: Intravenous, 50-200 mg/kg/day for 5 days	BALB/c: Significant reduction of viral titre; ~100-fold suppression of NP transcripts at 24 hpi at 40 mg/kg/day; ICR: Survival rates of 60% (200 mg/kg/day) and 30% (100 mg/kg/day); prolonged survival; reduced lung consolidation and improved pulmonary indices;	(Ding et al., 2014; Nayak et al., 2014)
Theaflavin-3′-gallate (TF2b)	BALB/c mice	15 MLD_{50} of mouse-adapted A/Changchun/01/2009 (H1N1)	Intraperitoneal, 50 mg/kg/day twice for 7 days	Alleviated body weight loss and significantly enhanced survival in lethally infected mice compared to controls and TF1-treated group	Sima et al. (2023)
Theaflavin (TF1)	BALB/c mice	15 MLD_{50} of m ouse-adapted A/Changchun/01/2009 (H1N1)	Intraperitoneal, 50 mg/kg/day twice for 7 days	Did not prevent infection-related body weight loss; no significant improvement in survival	Sima et al. (2023)
Kaempferol	BALB/c mice	1200 PFU of A/Puerto Rico/8/34 (H1N1)	Oral gavage, 3 and 30 mg/kg/day	Reduced viral titres in BALF and alleviated disease	Kai et al. (2014)
Kaempferol	BALB/c mice	6.8×10^3 PFU of A/WSN/33 (H1N1)	Intragastric, 100 mg/kg/day	Pretreatment worsened outcomes, accelerated mortality, severe lung injury, and enhanced viral dissemination to distal bronchi	Dong et al. (2014)
Hesperidin	BALB/c mice	6.8×10^3 PFU of A/WSN/33 (H1N1)	Intragastric, 100 mg/kg/day	Significantly improved survival and reduced lung pathology; NS1 and NP signals confined to superior segmental bronchus by day 3 versus widespread dissemination in controls	Dong et al. (2014)
Miquelianin (quercetin 3-O-glucuronide)	BALB/c mice	5 MLD_{50} of mouse-adapted A/Changchun/01/2009 (H1N1-UI182 variant)	Intragastric, 6 mg/kg/day for 5 days	Reduced IAV-induced lung inflammation and tissue damage; decreased proinflammatory cytokine production	Li et al. (2025)
Isorhamnetin	C57BL/6	5 MLD_{50} of A/Puerto Rico/8/34 (H1N1)	Oral, 1 mg/kg for 5 days	Reduced lung viral titre ~2-fold; improved survival to 70–80%; reduced body weight loss by 25%	Dayem et al. (2015)

*MLD_{50} = Median lethal dose.
*LD_{50} = Lethal dose required to kill 50% of the experimental population.
*$TCID_{50}$ = 50% tissue culture infectious dose.
*PFU = Plaque-forming units.

Complementary qRT-PCR and docking studies further indicated that Q7G may target the PB2 subunit, thereby suppressing viral RNA synthesis [Table 3] (Gansukh et al., 2016). In addition, isoquercetin, a naturally occurring quercetin glycoside, significantly suppressed viral replication when administered prior to infecting MDCK cells and maintained activity when added up to 4 h post-infection, pointing to an early-stage mechanism of action. Notably, intraperitoneal treatment with isoquercetin at 10 mg/kg/day markedly reduced lung viral titers in IAV-infected mice compared with untreated controls [Table 4] (Kim et al., 2010). Collectively, quercetin and its glycosylated derivatives represent promising antiviral candidates, particularly for targeting early in the course of influenza infection.

Bilobetin from *Euphorbia brevicornu* (African milk barrel), a biflavonoid with low cytotoxicity, exhibited strong inhibition of polymerase acidic protein (PA) endonuclease (PAN) activity in a gel-based assay, with an IC_{50} of 26.62 ± 8 μM. While these results are promising, further *in vitro* and *in vivo* studies are required to confirm its antiviral efficacy and therapeutic potential against diverse IAV strains (Zhang and Wang, 2021). In addition, theaflavin (TF1) and theaflavin-3′-gallate (TF2b), compounds derived from black tea, have demonstrated notable antiviral activity. TF1 and TF2b inhibited H1N1 and H3N2 IAV replication in MDCK and A549 cells, with EC_{50} values of 11.72 μg/mL and 8.45 μg/mL, respectively [Fig. 1 & Table 2]. IFA revealed a marked reduction in viral NP expression in treated cells, indicating that both compounds may interfere with viral replication and transcription [Fig. 1]. Moreover, *in vivo* experiments in BALB/c mice showed differential effects, TF1 did not prevent infection-related weight loss, whereas TF2b not only alleviated weight loss but also significantly enhanced survival in mice lethally infected with H1N1 compared with controls [Table 4] (Sima et al., 2023). These findings underscore the potential of TF2b as a more effective antiviral candidate among the two theaflavins. Another recent study identified Licoflavone B, a licorice-derived flavonoid, as a potent broad-spectrum anti-influenza agent that inhibits multiple IAV subtypes of H1N1 and H3N2 by targeting the viral RdRp. Western blotting and IFA data showed that the compound significantly suppressed viral replication, reduced NP and PB2 protein expression, and demonstrated favourable antiviral selectivity (IC_{50} = 6.7 μM) with low cytotoxicity in MDCK-Gluc cells [Table 2]. Molecular docking and mechanistic analyses suggested that Licoflavone B directly interacts with the viral polymerase complex, highlighting RdRp as its primary antiviral target. However, the

study was primarily limited to *in vitro* experiments, and therefore the *in vivo* antiviral efficacy, pharmacokinetics, and safety profile of Licoflavone B remain unclear [Table 3]. Additionally, although molecular docking suggested interaction with the viral RdRp complex, direct biochemical validation of the binding mechanism was not comprehensively established (Fan et al., 2025). Rhamnocitrin, another flavonoid, exhibits significant anti-IAV activity against H3N2 *in vitro*, with an IC_{50} value of 2.322 μM in MDCK cells [Table 2]. The compound suppressed viral replication, reduced NP expression, and attenuated virus-induced apoptosis and inflammatory responses in infected cells. However, the study was limited to *in vitro* experiments, and the precise antiviral target and stage-specific mechanism of inhibition remain unclear (Chen et al., 2024).

Tricin (4′,5,7-trihydroxy-3′,5′-dimethoxyflavone), a flavonoid derived from *Sasa senanensis* (Kumazasa), demonstrated promising antiviral effects, with IC_{50} values of 3.4 μM against H3N2 and 8.2 μM against H1N1 IAVs [Table 2]. In infected MDCK cells, it suppressed HA and M protein expression as well as their mRNAs, while exerting minimal influence on HI and NAI activity. In a DBA/2Cr mouse model, it significantly reduced body weight loss and prolonged survival [Table 4] (Yazawa et al., 2011). Several flavonoids isolated from *Scutellaria baicalensis* (Skullcap) have demonstrated potent anti-H1N1 IAV activity in MDCK cells. Among them, baicalein (IC_{50} = 7.5 μM), baicalin (7.4 μM), chrysin (7.7 μM), and oroxylin A (12.8 μM) showed notable effects, with wogonin exhibiting the strongest inhibition (IC_{50} = 2.1 μM) [Tables 1 and 2]. For comparison, oseltamivir phosphate displayed a considerably higher IC_{50} of 45.6 μM (Ji et al., 2015). Baicalin reduced IAV strain A/H1N1/Eastern India/66/pdm09 replication in A549 cells with an IC_{50} of ~18 μM (pfu assay, 72 h) and decreased viral titers both *in vitro* (10 μM) and *in vivo* (40 mg/kg/day) [Fig. 1 & Table 2]. Treatment led to ~100-fold suppression of NP transcripts at 24 hpi, and docking together with mutagenesis confirmed baicalin binding to the NS1 RNA-binding domain, particularly residues 39–43, indicating NS1 as a key antiviral target [Fig. 1 & Tables 2 and 3] (Nayak et al., 2014). Consistent with these results, another investigation revealed that baicalin inhibited replication of A/Jingfang/01/1986 (H1N1) and A/Lufang/09/1993 (H3N2) IAV strains in A549 cells by dose-dependently reducing NP and matrix protein (M1) protein expression, as verified by Western blotting (Li and Wang, 2019).

This body of evidence highlights that multiple flavonoids target the transcription–replication–translation axis of IAV, often through direct interactions with viral polymerase subunits (PB2, PA), regulatory proteins (NS1), or by disrupting host pathways essential for viral RNA synthesis. Compounds such as dihydromyricetin, baicalin, and quercetin derivatives demonstrate clear IAV specificity, reinforcing their promise as lead candidates. However, many studies remain limited to *in vitro* or small animal models, with inconsistent pharmacokinetic data and incomplete time-of-addition analyses, leaving gaps in mechanistic validation. Future work should prioritize systematic *in vivo* studies, detailed mechanistic confirmation, and optimisation of bioavailability to translate these flavonoids into clinically relevant antivirals.

2.5. Impact of flavonoids on IAV budding and release

In IAV infection, the final stages of the viral life cycle are critical for producing infectious virions and enabling viral dissemination. After the viral genome is replicated within the host nucleus, vRNPs are exported to the cytoplasm through a chromosome region maintenance-1 (CRM1)-mediated pathway, aided by viral proteins such as M1 and non-structural protein 2 (NS2). These vRNPs are directed to the apical membrane, where they contribute to the coordinated assembly of new virions. Subsequent virion maturation and release rely on NA activity, which removes sialic acid residues to ensure efficient detachment of budding virus particles (Dou et al., 2018; Rossman and Lamb, 2011). Given the importance of these critical events of IAV infection, several flavonoid compounds have been investigated for their potential to interfere with budding and release phase of the IAV life cycle.

Apigenin (4′,5,7-trihydroxyflavone), a flavonoid commonly found in Chinese medicinal plants, exhibits antiviral activity by suppressing NA function in a dose-dependent manner [Fig. 1, Tables 1, 2, and 5]. It demonstrated efficacy against IAV subtypes H1N1 and H3N2 in both MDCK and A549 cells (Liu et al., 2008; Xu et al., 2020). Similarly, flavonoids such as 5-hydroxy-6,7-dimethoxyflavone, 5-hydroxy-7,8-dimethoxyflavone, apigenin, and acacetin isolated from *Mosla scabra* (Mini-shiso) showed significant inhibition of A/PR/8/34H1N1 IAV replication in MDCK cells, with IC_{50} values ranging from 1.2 to 2.5 μg/mL [Table 2] (Wu et al., 2010). Interestingly, oseltamivir- and peramivir-resistant H1N1 IAV strains (A/Toyama/129/2011) remained susceptible to apigenin and kaempferol derived from Brazilian propolis, showing EC_{50} values (8.1 ± 4.7 to 38.2 ± 17.1 μg/mL) comparable to ribavirin (19.2 ± 7.5 μg/mL) [Table 2]. In a PRA, apigenin exhibited stronger antiviral activity than kaempferol (Kai et al., 2014). Additional cell-based studies revealed that kaempferol acts post-entry, suppressing replication without affecting viral adsorption or entry. *In vivo*, kaempferol significantly reduced viral titers in BALF and alleviated disease when administered intragastrically at 30 mg/kg in mice infected with A/PR/8/34 (H1N1) IAV [Table 4] (Kai et al., 2014). However, contrasting results were observed with a different H1N1 IAV strain (A/WSN/33), where pretreatment with kaempferol (100 mg/kg/day, 48 h before infection) worsened disease outcomes, resulting in earlier mortality and severe lung pathology. All treated animals succumbed by day 10, earlier than vehicle controls. Histopathological analysis on day 6 revealed severe lung injury, including tissue fragmentation, alveolar collapse, and infiltration of neutrophils, monocytes, and lymphocytes (Dong et al., 2014). Immunohistochemical staining for NS1 and NP proteins further demonstrated enhanced viral dissemination, with more extensive antigen detection in distal bronchi, indicating deeper and wider spread of infection in kaempferol-treated mice. However, mechanistic experiments required to define the exact cause has not been performed in this study (Dong et al., 2014). In contrast, hesperidin, a flavanone glycoside, exhibited strong antiviral effects both *in vitro* and *in vivo*. In MDCK cells, it reduced virion production by 148-fold and suppressed NS1 and NP expression, as demonstrated by $TCID_{50}$ and Western blot analyses. In infected mice, hesperidin significantly improved survival and reduced lung pathology compared with untreated or kaempferol-treated groups. By day 3 post-infection, NS1 and NP signals in hesperidin-treated mice were largely confined to the superior segmental bronchus, whereas control and kaempferol-treated animals showed widespread viral dissemination into distal bronchi (Dong et al., 2014). These findings highlight hesperidin as a promising flavonoid with superior antiviral efficacy, emphasizing that subtle structural differences among flavonoids critically influence their therapeutic potential against influenza.

C-methylated chalcone-type flavonoids isolated from *Cleistocalyx operculatus* buds showed notable NA inhibition against H1N1 and H9N2 IAVs, with IC_{50} values ranging from 18.6 to 85.7 μM [Table 5]. Among them, C-methylated flavonoid-4 displayed particularly strong effects, curtailing both wild-type and oseltamivir-resistant H1N1 (H274Y) NA with IC_{50} values of 8.2 and 3.3 μM in 293T cells [Table 5]. Although their potency was lower than oseltamivir, these chalcones retained activity against resistant variants, positioning them as valuable alternative therapies (Dao et al., 2010). Furthermore, a chalcone derivative—2′, 4′-dihydroxy-6′-methoxy-3′,5′-dimethylchalcone—and the flavonol glycoside myricetin-3′,5′-dimethylether 3-O-β-d-galactopyranoside from the same plant also potently inhibited influenza NAs, including H274Y mutants, with IC_{50} values between 5.07 and 9.34 μM in HEK293 cells [Table 5], and blocking H1N1 IAV replication in MDCK cells (Ha et al., 2016). However, further *in vitro* and *in vivo* studies are required to fully elucidate their inhibitory mechanisms against IAV. Isoliquiritigenin and echinantin, isolated from *Glycyrrhiza inflata* (Licorice), inhibited NAs from both wild-type and oseltamivir-resistant H1N1 IAVs expressed in 293T cells. Importantly, echinantin synergistically enhanced

Table 5
Inhibition of NA activity by various flavonoid compounds against influenza A subtypes H1N1 and H3N2.

Compound	Strain	IC50	Assay	Reference
Apigenin	A/PuertoRico/8/34 (H1N1)	8.55 ± 1.45 μM	NAI using MUNANA	Liu et al. (2008)
Luteolin	A/Jinan/15/90 (H3N2)	9.64 ± 1.83 μM	NAI using MUNANA	Liu et al. (2008)
C-methylated flavonoid 4	Oseltamivir resistant H1N1 (with H274Y mutation)	3.31 ± 1.34 μM	NAI using MUNANA	Dao et al. (2010)
	A/PuertoRico/8/34 (H1N1)	8.15 ± 1.05 μM		
C-methylated flavonoid 7	Oseltamivir resistant H1N1 (with H274Y mutation)	5.03 ± 0.87 μM	NAI using MUNANA	Dao et al. (2010)
	A/PuertoRico/8/34 (H1N1)	35.23 ± 2.75 μM		
C-methylated flavonoid 8	Oseltamivir resistant H1N1 (with H274Y mutation)	26.02 ± 3.03 μM	NAI using MUNANA	Dao et al. (2010)
	A/PuertoRico/8/34 (H1N1)	93.77 ± 5.35 μM		
C-methylated flavonoid 14	Oseltamivir resistant H1N1 (with H274Y mutation)	2.55 ± 0.29 μM	NAI using MUNANA	Dao et al. (2010)
	A/PuertoRico/8/34 (H1N1)	10 ± 2.17 μM		
Echinantin	Oseltamivir resistant H1N1 (with H274Y mutation)	2.19 ± 0.06 μg/mL	NAI using MUNANA	Dao et al. (2011)
	A/PuertoRico/8/34 (H1N1)	2.49 ± 0.14 μg/mL		
Isoliquiritigenin	Oseltamivir resistant H1N1 (with H274Y mutation)	3.42 ± 0.12 μg/mL	NAI using MUNANA	Dao et al. (2011)
	A/PuertoRico/8/34 (H1N1)	3.48 ± 0.19 μg/mL		
3-Deoxysappanchalcone	A/Puerto Rico/8/34 (PR8)	14.6 ± 0.2 μg/mL	NAI using MUNANA	Liu et al. (2009)
	A/Guangdong/243/72 (H3N2)	17.4 ± 0.9 μg/mL		
Sappanchalcone	A/Puerto Rico/8/34 (PR8)	14.3 ± 0.1 μg/mL	NAI using MUNANA	Liu et al. (2009)
	A/Guangdong/243/72 (H3N2)	21.2 ± 0.6 μg/mL		
Gossypetin	A/Bervig_Mission/1/18 (H1N1)	2.6 ± 1.1 μM	ELISA	Jeong et al. (2009)
Kaempferol	A/Bervig_Mission/1/18 (H1N1)	11.2 ± 1.0 μM	ELISA	Jeong et al. (2009)
2′,4′-dihydroxy-6′-methoxy-3′,5′-dimethylchalcone	A/Puerto Rico/8/34 (PR8)	8.23 ± 0.66 μM	NAI using MUNANA	Ha et al. (2016)
	Oseltamivir resistant H1N1 (with H274Y mutation)	8.84 ± 1.26 μM		
Myricetin-3′,5′-dimethylether 3-O-β-d-galactopyranoside	A/PuertoRico/8/34 (H1N1)	8.68 ± 1.39 μM		
	Oseltamivir resistant H1N1 (with H274Y mutation)	9.34 ± 2.52 μM		
Ginkgetin	A/PR/8/34 (H1N1)	55.00 μg/mL	NAI using MUNANA	Miki et al. (2007)
	A/Guizhou/54/89 (H3N2)	9.78 μg/mL		
5,7,4′-Trihydroxy-8-methoxyflavone	A/PR/8/34 (H1N1)	9.78 μg/mL	NAI using MUNANA	Miki et al. (2007)
	A/Guizhou/54/89 (H3N2)	8.95 μg/mL		
Agathisflavone	A/England/42/1972 (H3N2)	20.4 ± 2.6 μM	Cell- free assay	de Freitas et al. (2020)
	A/California/07/2009 (H1N1)	28.6 ± 1.7 μM		
	A/Texas/12/2007 (oseltamivir-resistant E119V, H3N2)	2.2 ± 0.58 μM		
	A/Florida/21/2008 (oseltamivir-resistant H275Y, H1N1)	3.5 ± 0.91 μM		
Baicalin	A/FM1/1/47 (H1N1)	52.3 μg/ml	NAI using MUNANA	Ding et al. (2014)
	A/Beijing/32/92 (H3N2)	85.8 μg/ml		
EGCG	A/Perth/25/2013 and A/Victoria/503/2013		NAI using MUNANA	Müller and Downard (2015)
Hispidulin	A/PR/8/34 (H1N1)	19.83 ± 2.28 μM	NAI using MUNANA	Bang et al. (2016)
Nepetin		11.18 ± 1.73 μM		
Luteolin		17.96 ± 2.38 μM		

*MUNANA = 2′-(4-methylumbelliferyl)-α-D-acetylneuraminic acid.
*NAI = Neuraminidase inhibition assay.
*IC50 = Denotes the concentration required to reduce enzyme activity by 50%.

oseltamivir's activity against the H274Y mutant, suggesting clinical relevance for drug-resistant influenza (Dao et al., 2011). Similarly, 3-deoxysappanchalcone (3-DSC) and sappanchalcone (SPC) from *Caesalpinia sappan* (Sappanwood) suppressed IAV replication, especially against H3N2, with IC_{50} values of 1.06 and 2.06 μg/mL in MDCK cells [Fig. 1 & Table 2]. They also inhibited NA activity from H1N1 and H3N2 IAVs (IC_{50}: 14–21 μg/mL), though less potently than oseltamivir (IC_{50}: 0.065 μg/mL) [Table 5] (Liu et al., 2009). At 30 μM, 3-DSC significantly downregulated NP expression in IAV-infected A549 cells, pointing toward partial interference with genome replication and transcription, though additional mechanisms may be involved (Yang et al., 2012).

Agathisflavone, isolated from *Anacardium occidentale*, also showed broad anti-IAV activity by inhibiting NA from both wild-type and oseltamivir-resistant strains, with IC_{50} values between 20 and 2.0 μM, while suppressing replication with an EC_{50} of 1.3 μM [Table 2 & Fig. 1]. Serial viral passaging under drug pressure revealed R253Q, A250S, and R249S substitutions in NA—mutations located outside the classical oseltamivir-binding site—indicating that agathisflavone likely targets a distinct NA region (de Freitas et al., 2020). Finally, hispidulin and nepetin from *Salvia plebeia* reduced CPE in H1N1 IAV-infected MDCK cells at concentrations of 17–20 μM [Fig. 1 & Table 2]. Along with luteolin, these flavonoids displayed moderate NA inhibition, with IC_{50} values between 11 and 19 μM [Tables 2 and 5] (Bang et al., 2016).

Moreover, baicalin was also shown to inhibit NA activity of both A/FM1/1/47 (H1N1) and A/Beijing/32/92 (H3N2) in a concentration-dependent manner [Fig. 1 & Table 5]. In animal models, baicalin provided substantial protection, with survival rates of 60% at 200 mg/kg/day and 30% at 100 mg/kg/day. Treated mice also exhibited prolonged survival, reduced lung consolidation, and improved pulmonary indices [Table 4] (Ding et al., 2014). EGCG displayed mild inhibitory effects on NA activity (Kim et al., 2013) and inhibited the NA activity (IC_{50}: 100.3 μM) of influenza strains A/Perth/25/2013 (H1N1) and

A/Victoria/503/2013 (H1N1) [Fig. 1 & Table 5] (Müller and Downard, 2015). Alongside EGCG, isorhamnetin—a methylated flavonol—has demonstrated notable antiviral activity by simultaneously targeting both HA and NA in MDCK cells and mouse models [Tables 1, 2, and 4]. This dual mechanism disrupts viral entry and hinders the release of progeny virions, ultimately suppressing the replication cycle (Dayem et al., 2015). Taken together, these findings suggest that both EGCG and isorhamnetin exert multi-target antiviral effects against influenza viruses, yet further mechanistic and pharmacokinetic studies are necessary to determine their translational potential for clinical use.

Further evidence of NA-targeting flavonoids comes from ginkgetin and 5,7,4′-trihydroxy-8-methoxyflavone, which inhibited sialidase activity of H1N1 and H3N2 IAVs, and their sialic acid conjugates also improved survival in infected mice (Miki et al., 2007). From *Salvia plebeian* (Sage weed), three flavonoids showed potent NA inhibition against H1N1 IAVs at 50 μM, surpassing oseltamivir phosphate tested at 100 μM, [Table 5] (Bang et al., 2018). Another potent phytocompound, gossypetin from *Rhodiola rosea* (Roseroot), strongly inhibited NA from the 1918 pandemic strain A/Brevig_Mission/1/1918 with an IC_{50} of 2.6 μM [Table 5] (Jeong et al., 2009).

Together, these findings highlight the chemical diversity of flavonoids as NA inhibitors, ranging from chalcones and flavonols to biflavones, and emphasize their potential as scaffolds for developing novel therapeutics against both drug-sensitive and drug-resistant influenza strains.

3. Improving flavonoid bioavailability for clinical translation

Clinical trial evidence in influenza has mainly involved flavonoid-containing botanical preparations, including elderberry extract (Sambucol) and Echinacea-based Echinaforce Hotdrink, rather than purified individual flavonoids (Rauš et al., 2015; Zakay-Rones et al., 2004). There is a notable lack of clinical data on purified flavonoids evaluated in human trials for influenza. Despite their broad-spectrum antiviral activity against IAV *in vitro* as well as *in vivo*, flavonoids face significant translational hurdles that constrain their clinical utility. Chief among these are poor aqueous solubility, extensive metabolism before reaching systemic circulation, rapid conjugation, and consequently low systemic bioavailability following oral administration. These pharmacokinetic limitations are particularly problematic in the context of influenza, where therapeutic efficacy depends on achieving sufficient drug concentrations at the respiratory mucosa and, in severe cases, maintaining sustained exposure within lung tissue. As a result, current research has shifted toward advanced formulation strategies designed to enhance stability, improve absorption, and enable targeted delivery to the respiratory tract, rather than relying on unmodified flavonoid compounds (Passamonti et al., 2009; Rios-Ibarra et al., 2024; Thilakarathna and Rupasinghe, 2013).

One major strategy is prodrug design, in which chemical modification temporarily masks polar groups to improve membrane permeability and oral uptake, followed by enzymatic conversion to the active parent compound *in vivo*. This approach is conceptually appealing for flavonoids such as quercetin, baicalin, and hesperidin, whose intrinsic antiviral potency can be undermined by poor absorption and extensive phase II metabolism (Biasutto and Zoratti, 2014). In parallel, nanoparticle-based delivery systems have gained considerable attention as practical solutions to overcome key limitations of flavonoids. These systems can enhance aqueous solubility, shield compounds from premature degradation, and enable controlled or site-specific release. Platforms such as liposomes, polymeric nanoparticles, and solid lipid nanoparticles have consistently demonstrated improvements in the pharmacokinetic profiles and therapeutic efficacy of flavonoids. As a result, nanocarrier-based approaches are increasingly viewed as a promising strategy to facilitate the translation of naturally derived antiviral compounds into clinically viable drug candidates (Ranjbar et al., 2023; Zverev and Rykunova, 2022).

For influenza specifically, local respiratory delivery may be especially valuable. Inhalation or intranasal formulations may concentrate flavonoids directly at the initial site of viral replication, potentially reducing the dose needed for efficacy while minimizing systemic exposure and metabolism. This is relevant because some flavonoids show antiviral effects *in vitro* but inconsistent *in vivo* performance, likely due to insufficient exposure at the site of infection. A research demonstrated that aerosol inhalation of luteolin-7-O-glucuronide significantly reduced pulmonary injury by inhibiting inflammatory infiltration and enhancing lung function in rat model of acute lung injury (Li et al., 2024). Another study developed solid lipid microparticles (SLMs) as dry powders containing quercetin for direct administration to the lung. Quercetin microparticles were prepared by oil-in-water emulsification using tristearin as the lipid component and phosphatidylcholine as an emulsifier. Although quercetin SLMs have been successfully formulated, their antiviral efficacy against IAV remains to be elucidated in relevant *in vivo* models (Scalia et al., 2013). Solid lipid nanoparticles also have been employed to overcome the bioavailability limitations of baicalin with optimized formulations demonstrating improved drug release profiles and enhanced cellular accumulation in Caco-2 cells (Ammar et al., 2023).Therefore, inhalable nanoformulations and other pulmonary delivery systems may offer a more realistic translational path than conventional oral dosing for poorly bioavailable flavonoids. Overall, future influenza research should integrate antiviral mechanism studies with formulation science, pharmacokinetic profiling, and respiratory delivery strategies to determine whether flavonoids can be advanced from promising lead compounds to clinically useful therapeutics.

4. Artificial intelligence as a transformative tool in anti-IAV phytocompound research

The integration of artificial intelligence (AI) and contemporary computational tools represents a transformative opportunity for advancing phytocompound-based anti-IAV drug discovery. Machine learning (ML) models trained on existing bioactivity datasets can now screen multi-million compound libraries with high throughput and mechanistic precision. Recent approaches including generative models and deep reinforcement learning are now capable of screening multi-million compound libraries with mechanistic precision; a recent demonstration employed deep reinforcement learning to generate over 60,000 novel NA-targeting candidates, identifying two compounds with confirmed *in vitro* and *in vivo* anti-IAV activity at low micromolar EC_{50} values and 65–100% murine protection, including against the oseltamivir-resistant H275Y NA mutant (Izmailyan et al., 2024). For phytocompounds specifically, whose structural diversity and multi-target pharmacology present formidable bottlenecks in target identification and synthetic optimisation, recurrent neural networks (RNN)-based generative models have already demonstrated the capacity to produce over 67 million structurally valid natural product-like molecules for high-throughput in silico screening (Tay et al., 2023). It is representing a 165-fold expansion of the accessible natural product chemical space, while AI algorithms that simultaneously assess multiple disease pathways and protein interactions are enabling the design of multi-target compounds that modulate several biological processes concurrently (Ai et al., 2024; Liu et al., 2025). The AlphaFold protein structure database, which contains more than 214 million predicted protein structures, offers high-confidence structural models for host proteins relevant to IAV. For proteins that lack experimentally resolved crystal structures, these models provide a practical basis for structure-based virtual screening of phytocompound libraries and expand opportunities to investigate host-directed targets that were previously difficult to assess for drug discovery (Varadi et al., 2024). Ultimately, the biological promise documented throughout this review will remain unrealised without a deliberate embrace of contemporary computational drug discovery approaches including AI-driven lead optimisation, structure-based virtual screening against

AlphaFold-resolved host targets, and machine learning-guided ADMET prediction, as the methodological standard for the next generation of phytocompound anti-IAV research.

5. Conclusion and future recommendations

This review brings together multiple studies showing that flavonoids interfere with multiple stages of the IAV life cycle. Compounds such as EGCG, quercetin derivatives, and dihydromyricetin act on viral entry or polymerase activity, while others like isorhamnetin, baicalin, and silybin derivatives affect HA, NA, or vRNP-associated processes. This breadth of activity illustrates the potential of flavonoids as scaffolds for multi-target antiviral strategies, particularly in the face of drug resistance.

However, despite potent *in vitro* efficacy, *in vivo* outcomes remain inconsistent, as highlighted by EGCG's variable effects across animal models and strain-dependent responses to kaempferol versus hesperidin. Challenges such as poor bioavailability, undefined *in vivo* mechanisms, and the need for standardized experimental approaches still limit translational progress. Moreover, most available findings stem from *in vitro* studies, with animal models as well as human data remaining sparse.

Ultimately, the integration of plant-derived compounds into the antiviral pipeline, either as standalone therapies or in combination with conventional antivirals holds great promise. Future research should prioritize mechanistic studies using appropriate animal models, pharmacokinetic and pharmacodynamic profiling, optimized formulations, especially for local respiratory delivery and combination studies with licensed antivirals to overcome resistance. Moreover, systematic mechanism-of-action studies, supported by structural biology and *in vivo* validation, are essential to establish target engagement and therapeutic relevance. Collectively, current findings suggest that flavonoids hold genuine promise as leads for next-generation influenza therapeutics, provided mechanistic clarity and rigorous *in vivo* validation are pursued. In addition, the integration of AI-driven computational tools, including structure-based virtual screening against AlphaFold-resolved viral and host targets, ML-guided ADMET optimisation, and generative models for multi-target scaffold design, offers a transformative and now accessible pathway to accelerate that progression from biological observation to clinically viable antiviral candidate.

Ethics approval and consent to participate

Not applicable.

Funding

Subir Sarker is the recipient of an Australian Research Council Discovery Early Career Researcher Award (grant number DE200100367) funded by theAustralian Government. The Australian Government had no role in the study design, data collection and analysis, decision to publish, or preparation of the manuscript. Phurpa Wangchuk is supported by the National Health and Medical Research Council (NHMRC) Ideas grant (APP, 2029349).

CRediT authorship contribution statement

Dibakar Chowdhury: Conceptualization, Formal analysis, Investigation, Methodology, Visualization, Writing – original draft. **Hillary A. Vanderven:** Conceptualization, Supervision, Validation, Writing – review & editing. **Phurpa Wangchuk:** Conceptualization, Supervision, Validation, Writing – review & editing. **Subir Sarker:** Conceptualization, Funding acquisition, Project administration, Resources, Software, Supervision, Validation, Writing – review & editing.

Declaration of competing interest

The authors declare that they have no known competing financial interests or personal relationships that could have appeared to influence the work reported in this paper.

Data availability

No data was used for the research described in the article.

References

AbuBakar, U., Low, Z.X., Aris, M.Z.M., Lani, R., Abidin, S.A.Z., Abdullah-Zawawi, M.R., Hassandarvish, P., Karsani, S.A., Khairat, J.E., 2025. Antiviral potential of diosmin against influenza A virus. Sci. Rep. 15 (1), 17192. https://doi.org/10.1038/s41598-025-00744-6.

Ai, C., Yang, H., Liu, X., Dong, R., Ding, Y., Guo, F., 2024. MTMol-GPT: de novo multi-target molecular generation with transformer-based generative adversarial imitation learning. PLoS Comput. Biol. 20 (6), e1012229.

Ammar, H.O., Shamma, R.N., Yousry, C., Elbatanony, R.S., Khater, B., Ghoneim, A.M., 2023. Characterization, cellular uptake in Caco-2 cells and physiologically based pharmacokinetic modeling of baicalin-loaded solid lipid nanoparticles. Future J. Pharmaceut. Sci. 9 (1), 61.

Bahramsoltani, R., Sodagari, H.R., Farzaei, M.H., Abdolghaffari, A.H., Gooshe, M., Rezaei, N., 2016. The preventive and therapeutic potential of natural polyphenols on influenza. Expert Review of Anti-Infective Therapy 14 (1), 57–80.

Bang, S., Ha, T.K.Q., Lee, C., Li, W., Oh, W.-K., Shim, S.H., 2016. Antiviral activities of compounds from aerial parts of Salvia plebeia R. Br. J. Ethnopharmacol. 192, 398–405.

Bang, S., Li, W., Ha, T.K.Q., Lee, C., Oh, W.K., Shim, S.H., 2018. Anti-influenza effect of the major flavonoids from Salvia plebeia R. Br. via inhibition of influenza H1N1 virus neuraminidase. Nat. Prod. Res. 32 (10), 1224–1228.

Beck, R., Ravet, M., Wieland, F., Cassel, D., 2009. The COPI system: molecular mechanisms and function. FEBS Lett. 583 (17), 2701–2709.

Beigel, J.H., Hayden, F.G., 2021. Influenza therapeutics in clinical practice—challenges and recent advances. Cold Spring Harb. Perspect. Med. 11 (4), a038463.

Biasutto, L., Zoratti, M., 2014. Prodrugs of quercetin and resveratrol: a strategy under development. Curr. Drug Metabol. 15 (1), 77–95. https://doi.org/10.2174/1389200214666131211160005.

Chen, C., Zhen-You, J., Bin, Y., Xian-Lin, W., Cong-Qi, D., Chang-Lin, Z., Da-Hong, J., Chen, X.-Y., 2012. Study on the anti-H1N1 virus effects of quercetin and oseltamivir and their mechanism related to TLR7 pathway. J. Asian Nat. Prod. Res. 14 (9), 877–885. https://doi.org/10.1080/10286020.2012.702108.

Chen, Z., Wang, W., Zeng, K., Zhu, J., Wang, X., Huang, W., 2024. Potential antiviral activity of rhamnocitrin against influenza virus H3N2 by inhibiting cGAS/STING pathway in vitro. Sci. Rep. 14 (1), 28287. https://doi.org/10.1038/s41598-024-79788-z.

Cho, W.K., Choi, H.J., Ahmad, S.S., Choi, I., Ma, J.Y., 2024. Antiviral effect of amentoflavone against influenza viruses. Int. J. Mol. Sci. 25 (22). https://doi.org/10.3390/ijms252212426.

Choi, H.J., Song, J.H., Park, K.S., Kwon, D.H., 2009. Inhibitory effects of quercetin 3-rhamnoside on influenza A virus replication. Eur. J. Pharmaceut. Sci. 37 (3–4), 329–333.

Choi, J.-G., Lee, H., Hwang, Y.-H., Lee, J.-S., Cho, W.-K., Ma, J.Y., 2017. Eupatorium fortunei and its components increase antiviral immune responses against RNA viruses. Front. Pharmacol. 8, 511.

Colpitts, C.C., Schang, L.M., 2014. A small molecule inhibits virion attachment to heparan sulfate-or sialic acid-containing glycans. J. Virol. 88 (14), 7806–7817.

Cureton, D.K., Burdeinick-Kerr, R., Whelan, S.P., 2012. Genetic inactivation of COPI coatomer separately inhibits vesicular stomatitis virus entry and gene expression. J. Virol. 86 (2), 655–666.

Dai, J.-P., Wu, L.-Q., Li, R., Zhao, X.-F., Wan, Q.-Y., Chen, X.-X., Li, W.-Z., Wang, G.-F., Li, K.-S., 2013. Identification of 23-(S)-2-Amino-3-Phenylpropanoyl-Silybin as an antiviral agent for influenza A virus infection in vitro and in vivo. Antimicrob. Agents Chemother. 57 (9), 4433–4443. https://doi.org/10.1128/aac.00759-13.

Dao, T.-T., Tung, B.-T., Nguyen, P.-H., Thuong, P.-T., Yoo, S.-S., Kim, E.-H., Kim, S.-K., Oh, W.-K., 2010. C-methylated flavonoids from cleistocalyx operculatus and their inhibitory effects on novel influenza A (H1N1) neuraminidase. J. Nat. Prod. 73 (10), 1636–1642.

Dao, T.T., Nguyen, P.H., Lee, H.S., Kim, E., Park, J., Lim, S.I., Oh, W.K., 2011. Chalcones as novel influenza A (H1N1) neuraminidase inhibitors from Glycyrrhiza inflata. Bioorg. Med. Chem. Lett 21 (1), 294–298.

Dayem, A.A., Choi, H.Y., Kim, Y.B., Cho, S.-G., 2015. Antiviral effect of methylated flavonol isorhamnetin against influenza. PLoS One 10 (3), e0121610.

de Freitas, C.S., Rocha, M.E., Sacramento, C.Q., Marttorelli, A., Ferreira, A.C., Rocha, N., de Oliveira, A.C., de Oliveira Gomes, A.M., Dos Santos, P.S., da Silva, E.O., 2020. Agathisflavone, a biflavonoid from Anacardium occidentale L., inhibits influenza virus neuraminidase. Curr. Top. Med. Chem. 20 (2), 111–120.

Derksen, A., Hensel, A., Hafezi, W., Herrmann, F., Schmidt, T.J., Ehrhardt, C., Ludwig, S., Kühn, J., 2014. 3-O-galloylated procyanidins from Rumex acetosa L. inhibit the attachment of influenza A virus. PLoS One 9 (10), e110089.

Ding, Y., Dou, J., Teng, Z., Yu, J., Wang, T., Lu, N., Wang, H., Zhou, C., 2014. Antiviral activity of baicalin against influenza A (H1N1/H3N2) virus in cell culture and in mice and its inhibition of neuraminidase. Arch. Virol. 159 (12), 3269–3278.
Dong, W., Wei, X., Zhang, F., Hao, J., Huang, F., Zhang, C., Liang, W., 2014. A dual character of flavonoids in influenza A virus replication and spread through modulating cell-autonomous immunity by MAPK signaling pathways. Sci. Rep. 4 (1), 7237.
Dou, D., Revol, R., Östbye, H., Wang, H., Daniels, R., 2018. Influenza A virus cell entry, replication, virion assembly and movement. Front. Immunol. 9, 1581.
El Sayed, K.A., 2000. Natural products as antiviral agents. Stud. Nat. Prod. Chem. 24, 473–572.
Fan, P., Lv, P., Zhang, S., Zhu, Z., Qian, K., Han, J., Cui, Y., Feng, Y., Li, Z., Qiang, L., Dong, Y., Fang, T., Jiang, T., Yu, C., Chi, X., 2025. Licoflavone B suppresses influenza A virus by targeting the viral RNA-dependent RNA polymerase (RdRp). Viruses 17 (9). https://doi.org/10.3390/v17091157.
Gabriely, G., Kama, R., Gerst, J.E., 2007. Involvement of specific COPI subunits in protein sorting from the late endosome to the vacuole in yeast. Mol. Cell Biol. 27 (2), 526–540.
Gansukh, E., Kazibwe, Z., Pandurangan, M., Judy, G., Kim, D.H., 2016. Probing the impact of quercetin-7-O-glucoside on influenza virus replication influence. Phytomedicine 23 (9), 958–967.
Ha, T.K.Q., Dao, T.T., Nguyen, N.H., Kim, J., Kim, E., Cho, T.O., Oh, W.K., 2016. Antiviral phenolics from the leaves of cleistocalyx operculatus. Fitoterapia 110, 135–141.
Hanada, A., Morimoto, R., Horio, Y., Shichiri, M., Nakashima, A., Ogawa, T., Suzuki, K., Sumitani, H., Ogata, T., Isegawa, Y., 2022. Influenza virus entry and replication inhibited by 8-prenylnaringenin from Citrullus lanatus var. citroides (wild watermelon). Food Sci. Nutr. 10 (3), 926–935.
Intharuksa, A., Kuljarusnont, S., Sasaki, Y., Tungmunnithum, D., 2024. Flavonoids and other polyphenols: bioactive molecules from traditional medicine recipes/medicinal plants and their potential for phytopharmaceutical and medical application. Molecules 29 (23). https://doi.org/10.3390/molecules29235760.
Ison, M.G., Hayden, F.G., Hay, A.J., Gubareva, L.V., Govorkova, E.A., Takashita, E., McKimm-Breschkin, J.L., 2021. Influenza polymerase inhibitor resistance: assessment of the current state of the art-A report of the isirv antiviral group. Antivir. Res. 194, 105158.
Izmailyan, R., Matevosyan, M., Khachatryan, H., Shavina, A., Gevorgyan, S., Ghazaryan, A., Tirosyan, I., Gabrielyan, Y., Ayvazyan, M., Martirosyan, B., 2024. Discovery of new antiviral agents through artificial intelligence: in vitro and in vivo results. Antivir. Res. 222, 105818.
Jeong, H.J., Ryu, Y.B., Park, S.-J., Kim, J.H., Kwon, H.-J., Kim, J.H., Park, K.H., Rho, M.-C., Lee, W.S., 2009. Neuraminidase inhibitory activities of flavonols isolated from Rhodiola rosea roots and their in vitro anti-influenza viral activities. Bioorg. Med. Chem. 17 (19), 6816–6823.
Ji, S., Li, R., Wang, Q., Miao, W.-j., Li, Z.-w., Si, L.-l., Qiao, X., Yu, S.-w., Zhou, D.-m., Ye, M., 2015. Anti-H1N1 virus, cytotoxic and Nrf2 activation activities of chemical constituents from Scutellaria baicalensis. J. Ethnopharmacol. 176, 475–484.
Kai, H., Obuchi, M., Yoshida, H., Watanabe, W., Tsutsumi, S., Park, Y.K., Matsuno, K., Yasukawa, K., Kurokawa, M., 2014. In vitro and in vivo anti-influenza virus activities of flavonoids and related compounds as components of Brazilian propolis (AF-08). J. Funct.Foods 8, 214–223.
Keshavarz, M., Ghorbani, M., Shamsizadeh, F., Namdari, H., Salimi, V., Rezaei, F., 2025. Effects and mechanisms of silibinin on influenza A/H1N1 pathogenesis in a mouse model. J. Trop. Med. 2025 (1), 6618423.
Kim, M., Kim, S.-Y., Lee, H.W., Shin, J.S., Kim, P., Jung, Y.-S., Jeong, H.-S., Hyun, J.-K., Lee, C.-K., 2013. Inhibition of influenza virus internalization by (−)-epigallocatechin-3-gallate. Antivir. Res. 100 (2), 460–472.
Kim, Y., Narayanan, S., Chang, K.-O., 2010. Inhibition of influenza virus replication by plant-derived isoquercetin. Antivir. Res. 88 (2), 227–235.
Kim, H.-K., Park, K.-J.J., 2012. A new efficient synthesis of oseltamivir phosphate (Tamiflu) from (−)-shikimic acid. Tetrahedron Lett. 53 (13), 1561–1563.
Kumar, S., Pandey, A.K., 2013. Chemistry and biological activities of flavonoids: an overview. Sci. World J. 2013 (1), 162750.
Li, H., Shen, B., Bi, Y., Sun, Y., Zhang, S., Xue, K., Wang, Q., Qian, B., Zhang, J., Fan, L., 2025. Miquelianin inhibits IAV infection via the MAPK signaling pathway both in vitro and in vivo. Front. Immunol. 16, 1532336.
Li, J., Song, L., Li, H., Gao, Y., Chen, T., Zhang, Z., Hon, H., Ye, Z., Zhang, G., 2024. Aerosol inhalation of Luteolin-7-O-Glucuronide exerts anti-inflammatory effects by inhibiting NLRP3 inflammasome activation. Pharmaceuticals 17 (12). https://doi.org/10.3390/ph17121731.
Li, R., Wang, L., 2019. Baicalin inhibits influenza virus A replication via activation of type I IFN signaling by reducing miR-146a. Mol. Med. Rep. 20 (6), 5041–5049.
Ling, J.-x., Wei, F., Li, N., Li, J.-l., Chen, L.-j., Liu, Y.-y., Luo, F., Xiong, H.-r., Hou, W., Yang, Z.-q., 2012. Amelioration of influenza virus-induced reactive oxygen species formation by epigallocatechin gallate derived from green tea. Acta Pharmacol. Sin. 33 (12), 1533–1541.
Liu, A.-L., Liu, B., Qin, H.-L., Lee, S.M.Y., Wang, Y.-T., Du, G.-H., 2008. Anti-influenza virus activities of flavonoids from the medicinal plant Elsholtzia rugulosa. Planta Med. 74 (8), 847–851.
Liu, A.-L., Shu, S.-H., Qin, H.-L., Lee, S.M.Y., Wang, Y.-T., Du, G.-H., 2009. In vitro anti-influenza viral activities of constituents from Caesalpinia sappan. Planta Med. 75 (4), 337–339.
Liu, Y., Qin, K., Meng, G., Zhang, J., Zhou, J., Zhao, G., Luo, M., Zheng, X., 2013. Structural and functional characterization of K339T substitution identified in the PB2 subunit cap-binding pocket of influenza A virus. J. Biol. Chem. 288 (16), 11013–11023.
Liu, Y.T., Zhang, L.L., Jiang, Z.Y., Tian, X.S., Li, P.L., Wu, P.H., Du, W.T., Yuan, B.Y., Xie, C., Bu, G.L., 2025. Applications of artificial intelligence in biotech drug discovery and product development. MedComm 6 (8), e70317.
Mehrbod, P., Abdalla, M.A., Fotouhi, F., Heidarzadeh, M., Aro, A.O., Eloff, J.N., McGaw, L.J., Fasina, F.O., 2018. Immunomodulatory properties of quercetin-3-O-α-L-rhamnopyranoside from Rapanea melanophloeos against influenza a virus. BMC Compl. Alternative Med. 18 (1), 184.
Middleton Jr, E., 1998. Effect of plant flavonoids on immune and inflammatory cell function. Flavonoids in the living system 175–182.
Miki, K., Nagai, T., Suzuki, K., Tsujimura, R., Koyama, K., Kinoshita, K., Furuhata, K., Yamada, H., Takahashi, K., 2007. Anti-influenza virus activity of biflavonoids. Bioorg. Med. Chem. Lett 17 (3), 772–775.
Müller, P., Downard, K.M., 2015. Catechin inhibition of influenza neuraminidase and its molecular basis with mass spectrometry. J. Pharmaceut. Biomed. Anal. 111, 222–230.
Morimoto, R., Hanada, A., Matsubara, C., Horio, Y., Sumitani, H., Ogata, T., Isegawa, Y., 2023. Anti-influenza A virus activity of flavonoids in vitro: a structure–activity relationship. J. Nat. Med. 77 (1), 219–227.
Morimoto, R., Matsubara, C., Hanada, A., Omoe, Y., Ogata, T., Isegawa, Y., 2022. Effect of structural differences in naringenin, prenylated naringenin, and their derivatives on the anti-influenza virus activity and cellular uptake of their flavanones. Pharmaceuticals 15 (12). https://doi.org/10.3390/ph15121480.
Mou, Q., Jiang, Y., Zhu, L., Zhu, Z., Ren, T., 2020. EGCG induces β-defensin 3 against influenza A virus H1N1 by the MAPK signaling pathway. Exp. Ther. Med. 20 (4), 3017–3024. https://doi.org/10.3892/etm.2020.9047.
Nayak, M.K., Agrawal, A.S., Bose, S., Naskar, S., Bhowmick, R., Chakrabarti, S., Sarkar, S., Chawla-Sarkar, M., 2014. Antiviral activity of baicalin against influenza virus H1N1-pdm09 is due to modulation of NS1-mediated cellular innate immune responses. J. Antimicrob. Chemother. 69 (5), 1298–1310.
Orders, M., 2024. Antiviral drugs for seasonal influenza for 2024-2025. Med. Lett. Drugs Ther. 66 (1717), 193–198.
Panche, A.N., Diwan, A.D., Chandra, S.R., 2016. Flavonoids: an overview. Journal of nutritional science 5, e47.
Passamonti, S., Terdoslavich, M., Franca, R., Vanzo, A., Tramer, F., Braidot, E., Petrussa, E., Vianello, A., 2009. Bioavailability of flavonoids: a review of their membrane transport and the function of bilitranslocase in animal and plant organisms. Curr. Drug Metabol. 10 (4), 369–394. https://doi.org/10.2174/138920009788498950.
Ranjbar, S., Emamjomeh, A., Sharifi, F., Zarepour, A., Aghaabbasi, K., Dehshahri, A., Sepahvand, A.M., Zarrabi, A., Beyzaei, H., Zahedi, M.M., Mohammadinejad, R., 2023. Lipid-based delivery systems for flavonoids and Flavonolignans: liposomes, nanoemulsions, and solid lipid nanoparticles. Pharmaceutics 15 (7). https://doi.org/10.3390/pharmaceutics15071944.
Rauš, K., Pleschka, S., Klein, P., Schoop, R., Fisher, P., 2015. Effect of an echinacea-based hot drink versus oseltamivir in influenza treatment: a randomized, double-blind, double-dummy, multicenter, noninferiority clinical trial. Curr. Ther. Res. Clin. Exp. 77, 66–72. https://doi.org/10.1016/j.curtheres.2015.04.001.
Rauter, A.P., Ennis, M., Hellwich, K.-H., Herold, B.J., Horton, D., Moss, G.P., Schomburg, I., 2018. Nomenclature of flavonoids (IUPAC recommendations 2017). Pure Appl. Chem. 90 (9), 1429–1486.
Raza, M.A., Ashraf, M.A., 2024. Drug resistance and possible therapeutic options against influenza A virus infection over past years. Arch. Microbiol. 206 (12), 458. https://doi.org/10.1007/s00203-024-04181-3.
Rios-Ibarra, C.P., Salinas-Santander, M., Orozco-Nunnelly, D.A., Bravo-Madrigal, J., 2024. Nanoparticle-based antiviral strategies to combat the influenza virus. Biomed Rep 20 (4), 65. https://doi.org/10.3892/br.2024.1753 (Review).
Rossman, J.S., Lamb, R.A., 2011. Influenza virus assembly and budding. Virology 411 (2), 229–236.
Sadati, S.M., Gheibi, N., Ranjbar, S., Hashemzadeh, M.S., 2019. Docking study of flavonoid derivatives as potent inhibitors of influenza H1N1 virus neuraminidase. Biomedical reports 10 (1), 33–38.
Scalia, S., Haghi, M., Losi, V., Trotta, V., Young, P.M., Traini, D., 2013. Quercetin solid lipid microparticles: a flavonoid for inhalation lung delivery. Eur. J. Pharmaceut. Sci. 49 (2), 278–285.
Shanks, G.D., 2015. Insights from unusual aspects of the 1918 influenza pandemic. Trav. Med. Infect. Dis. 13 (3), 217–222.
Sima, M., Lv, C., Qi, J., Guo, J., Luo, R., Deng, X., Li, Y., Wang, T., Yue, D., Gao, Y., 2023. Anti-inflammatory effects of theaflavin-3′-gallate during influenza virus infection through regulating the TLR4/MAPK/p38 pathway. Eur. J. Pharmacol. 938, 175332.
Song, J., Choi, H., 2011. Silymarin efficacy against influenza A virus replication. Phytomedicine 18 (10), 832–835.
Stannard, H., Koszalka, P., Deshpande, N., Desjardins, Y., Baz, M., 2023. Pre-clinical evaluation of the antiviral activity of epigalocatechin-3-gallate, a component of green tea, against influenza a (H1N1) pdm viruses. Viruses 15 (12), 2447.
Su, S., Gu, M., Liu, D., Cui, J., Gao, G.F., Zhou, J., Liu, X., 2017. Epidemiology, evolution, and pathogenesis of H7N9 influenza viruses in five epidemic waves since 2013 in China. Trends Microbiol. 25 (9), 713–728.
Tay, D.W., Yeo, N.Z., Adaikkappan, K., Lim, Y.H., Ang, S.J., 2023. 67 million natural product-like compound database generated via molecular language processing. Sci. Data 10 (1), 296.
Thilakarathna, S.H., Rupasinghe, H.P., 2013. Flavonoid bioavailability and attempts for bioavailability enhancement. Nutrients 5 (9), 3367–3387. https://doi.org/10.3390/nu5093367.
Tian, Y., Sang, H., Liu, M., Chen, F., Huang, Y., Li, L., Liu, S., Yang, J., 2020. Dihydromyricetin is a new inhibitor of influenza polymerase PB2 subunit and

influenza-induced inflammation. Microb. Infect. 22 (6), 254–262. https://doi.org/10.1016/j.micinf.2020.05.021.
Varadi, M., Bertoni, D., Magana, P., Paramval, U., Pidruchna, I., Radhakrishnan, M., Tsenkov, M., Nair, S., Mirdita, M., Yeo, J., 2024. AlphaFold protein structure database in 2024: providing structure coverage for over 214 million protein sequences. Nucleic Acids Res. 52 (D1), D368–D375.
WHO, 2025. Influenza seasonal. https://www.who.int/en/news-room/fact-sheets/detail/influenza-(seasonal).
Wu, Q., Yu, C., Yan, Y., Chen, J., Zhang, C., Wen, X., 2010. Antiviral flavonoids from Mosla scabra. Fitoterapia 81 (5), 429–433.
Wu, W., Li, R., Li, X., He, J., Jiang, S., Liu, S., Yang, J., 2015. Quercetin as an antiviral agent inhibits influenza A virus (IAV) entry. Viruses 8 (1), 6.
Xu, M.J., Liu, B.J., Wang, C.L., Wang, G.H., Tian, Y., Wang, S.H., Li, J., Li, P.Y., Zhang, R. H., Wei, D., Tian, S.F., Xu, T., 2017. Epigallocatechin-3-gallate inhibits TLR4 signaling through the 67-kDa laminin receptor and effectively alleviates acute lung injury induced by H9N2 swine influenza virus. Int. Immunopharmacol. 52, 24–33. https://doi.org/10.1016/j.intimp.2017.08.023.
Xu, X., Miao, J., Shao, Q., Gao, Y., Hong, L., 2020. Apigenin suppresses influenza A virus-induced RIG-I activation and viral replication. J. Med. Virol. 92 (12), 3057–3066.
Yan, H., Ma, L., Wang, H., Wu, S., Huang, H., Gu, Z., Jiang, J., Li, Y., 2019. Luteolin decreases the yield of influenza A virus in vitro by interfering with the coat protein I complex expression. J. Nat. Med. 73 (3), 487–496.
Yan, H., Wang, H., Ma, L., Ma, X., Yin, J., Wu, S., Huang, H., Li, Y., 2018. Cirsimaritin inhibits influenza A virus replication by downregulating the NF-κB signal transduction pathway. Virol. J. 15 (1), 88.
Yang, F., Zhou, W.-L., Liu, A.-L., Qin, H.-L., Lee, S.M.-Y., Wang, Y.-T., Du, G.-H., 2012. The protective effect of 3-deoxysappanchalcone on in vitro influenza virus-induced apoptosis and inflammation. Planta Med. 78 (10), 968–973.
Yang, Z.-F., Bai, L.-P., Huang, W.-b., Li, X.-Z., Zhao, S.-S., Zhong, N.-S., Jiang, Z.-H., 2014. Comparison of in vitro antiviral activity of tea polyphenols against influenza A and B viruses and structure–activity relationship analysis. Fitoterapia 93, 47–53.
Yazawa, K., Kurokawa, M., Obuchi, M., Li, Y., Yamada, R., Sadanari, H., Matsubara, K., Watanabe, K., Koketsu, M., Tuchida, Y., 2011. Anti-influenza virus activity of tricin, 4′, 5, 7-trihydroxy-3′, 5′-dimethoxyflavone. Antiviral Chem. Chemother. 22 (1), 1–11.
Zakay-Rones, Z., Thom, E., Wollan, T., Wadstein, J., 2004. Randomized study of the efficacy and safety of oral elderberry extract in the treatment of influenza A and B virus infections. J. Int. Med. Res. 32 (2), 132–140.
Zhang, J., Wang, Y., 2021. Bilobetin, a novel small molecule inhibitor targeting influenza virus polymerase acidic (PA) endonuclease was screened from plant extracts. Nat. Prod. Res. 35 (24), 5968–5971.
Zumdick, S., Deters, A., Hensel, A., 2012. In vitro intestinal transport of oligomeric procyanidins (DP 2 to 4) across monolayers of Caco-2 cells. Fitoterapia 83 (7), 1210–1217.
Zverev, Y.F., Rykunova, A.Y., 2022. Modern nanocarriers as a factor in increasing the bioavailability and pharmacological activity of flavonoids. Appl. Biochem. Microbiol. 58 (9), 1002–1020. https://doi.org/10.1134/s0003683822090149.